PROMICON

Collection, pre-screening and characterization of natural microbiomes

Deliverable D2.1

28 February 2022

Cristiana A.V. Torres[1], Marta Catalão[1], Filomena Freitas[1], Maria A.M. Reis[1]
Eva Gonzalez-Flo[2], Beatriz Altamira-Algarra[2], Marta Bellver-Catalá[2], Joan Garcia[2]

[1]Biochemical Engineering Group, Chemistry Department, School of Sciences and Technology, NOVA University of Lisbon (FCT NOVA), Associação para a Inovação e Desenvolvimento da FCT NOVA

[2]GEMMA-Group of Environmental Engineering and Microbiology, Department of Civil and Environmental Engineering, Universitat Politècnica de Catalunya-BarcelonaTech

PROMICOM

Harnessing the power of nature through PROductive MIcrobial CONsortia in biotechnology - measure, model, master

This project receives funding from the European Union's Horizon 2020 research and innovation programme under grant agreement No 101000733.

Prepared under contract from the European Commission

Grant agreement No. 101000733
EU Horizon 2020 Research and Innovation action

Project acronym:	**PROMICON**
Project full title:	**Harnessing the power of nature through PROductive MIcrobial CONsortia in biotechnology - measure, model, master**
Start of the project:	June 2021
Duration:	48 months
Project coordinator:	Dr. rer. nat. Jens O. Krömer Helmholtz Centre for Environmental Research - UFZ https://www.ufz.de/
Deliverable title:	Collection, pre-screening and characterization of natural microbiomes
Deliverable n°:	D2.1
Nature of the deliverable:	Report
Dissemination level:	Public
WP responsible:	WP2
Lead beneficiary:	NOVAID
Citation:	Torres, C.A.V., Catalão, M., Freitas, F., Reis, M.A.M., Gonzalez-Flo, E., Altamira-Algarra, B., Bellver-Catalá, M., Garcia, J. (2022). *Collection, pre-screening and characterization of natural microbiomes*. Deliverable D2.1 EU Horizon 2020 PROMICON Project, Grant agreement No 101000733.
Due date of deliverable:	Month nº9
Actual submission date:	Month n°9

Deliverable status:

Version	*Status*	*Date*	*Author(s)*
1.0	Final	15 March 2022	NOVA.id

Table of contents

Preface

WP2 “Natural Consortia for Learning and Production” has as its main objectives to develop and cultivate existing microbiomes from natural or artificial/industrial environments in highly controlled and optimized bioreactors for production of extracellular polysaccharides (EPS), polyhydroxyalkanoates (PHA) and phycobiliprotein pigments (PPP). More specifically, in Task 2.1, the NOVA.id partner has collected seven environmental samples originating from two different geographical areas, and encompassing distinct habitats, namely, forest soil, river sediments and plant roots. Each environmental sample was subjected to a selective pressure, aiming to select for PHA-accumulating microorganisms. The selected microbiomes were also evaluated for their EPS secreting ability. The microbiomes, both the environmental collected samples and those obtained during the selection assays, were characterized for their phenotypic and genotypic potential for the production of PHA and EPS. The UPC partner has collected several environmental samples that have been pre-cultured and characterized in terms of physicochemical and morphological properties of the organisms. To develop microbiomes rich in cyanobacteria from the collected environmental samples, a selective pressure process was applied, which allowed to select cyanobacteria microorganisms over other phototrophs such as green algae. From the obtained cyanobacteria microbiomes, their phenotypic and genotypic potential were characterized for the production of PHA, PPP and EPS.

List of abbreviations

Ac	Acetate
ANOVA	Analysis of variance
APC	Allophycocyanin
Ara	Arabinose
ASV	Amplicon Sequence Variant
Chla	Chlorophyl a
CW	Constructed wetland
DNA	Deoxyribonucleic acid
EPS	Exopolysaccharide/ Extracellular Polysaccharides
EU	European Union
FISH	Fluorescent in Situ Hybridization
FITC	Fluorescein isothiocyanate Fluorescein isothiocyanate
Fru	Fructose
Fuc	Fucose
Gal	Galactose
Glc	Glucose
GlcA	Glucuronic acid
GlcN	Glucosamine
GC	Gas Chromatography
HB	Hydroxybutyrate
HPLC	High Performance Liquid Chromatography
HV	Hydroxyvalerate
ICP-AES	Inductively Coupled Plasma – Atomic Emission Spectrometry
LCBD	Local contributions to beta diversity
Man	Mannose
NCBI	National Center for Biotechnology Information
OD	Optical density
PC	Phycocyanin
PE	Phycoerythrin
PHA	Polyhydroxyalkanoates
PPP	Phycobiliprotein Pigments

rRNA	Ribosomal ribonucleic acid
TFA	Trifluoroacetic acid
TSS	Total Suspended Solids
UP	Urban pond
VFA	Volatile Fatty Acid
VSS	Volatile Suspended Solids

1 Natural Heterotrophic Microbiomes

1.1 Environmental samples collection and site characterization

Seven sites from two main areas (Setúbal and Aveiro) were chosen to collect the environmental samples (Figure 1). These areas are exposed to different environmental and climate conditions. Roots from the fern *Dicksonia antartica* and from lima bean (*Phaseolus lunatus*), as well as forest soil from Mata Nacional do Buçaco, were collected in Aveiro region. The remaining samples were collected at the region of Setúbal, namely, in Caparica, Porto Brandão and Corroios. Roots from the beach dunes plant *Carpobrotus edulis* and forest soil from Mata Nacional dos Medos were collected from Caparica, while sediments were collected from the Tagus River mouth, in Porto Brandão, and from the marshlands, in Corroios. The soil (~500 g) and root (~250 g) samples were collected into clean bags, while the sediments (~1 L) were collected into clean flasks. All the samples were stored at 4 ºC and processed within 24 h after collection.

Figure 1: Geographic location of the sites for environmental samples collection for heterotrophic microbiomes: in the Aveiro region, soil samples were collected from Mata Nacional do Buçaco forest, as well as the roots of the fern *Dicksonia antartica* growing in the forest and of the lima bean *Phaseolus lunatus* growing in a home vegetable garden; in the Setúbal region, samples were collected at Caparica and Corroios, namely, soil samples at Mata Nacional dos Medos forest, roots from the beach dune plant *Carpobrotus edulis*, and river sediments at the Tagus mouth, all at Caparica, and sediments from Tagus estuarine marshland at Corroios.

The collection site of the fern roots and the soil from Mata do Buçaco is an ancient forest characterized by a prevailing microclimate with mild temperatures, frequent morning fog and precipitation almost double the regional average, that harbours hundreds of different species, including centenarian plants, as well as exotics ones originating from other continents. The lima bean roots were collected from a home vegetable garden in the rural part of Aveiro region.

The Caparica region is characterized by warm and temperate climate, in which there is low rainfall during the wintertime. The dune plant *Carpobrotus edulis* is an invasive species that grows extensively on several locations across the Portuguese Coast. Its roots were collected from the sand dunes, at Praia da Saúde beach, a dry and salt-containing habitat. Mata Nacional dos Medos, located in the upper platform of the Fossil Arriba of Costa da Caparica, is an extensive area of pine forest, with centenary pines and a botanical reserve with great richness and diversity of autochthonous species. The soil sample was collected from the surroundings of a pine tree.

The Tagus Estuary is a transitional aquatic environment between the Tagus River and the Atlantic Ocean. It separates Lisbon from the Setúbal Peninsula. It is the largest wetland in the country and one of the most important in Europe, a sanctuary for fish, molluscs, crustaceans and migratory birds. Porto Brandão is a small village at the left bank of the river, by the river mouth, where the ocean and river waters mix. It is subjected to considerable pollution due to the navigation of ships. The Corroios Marshland is the best-preserved wetland in the Tagus estuary, with a rich ornithological and aquatic fauna. It is an ecosystem with the capacity to store and sequester heavy metals, along with the roots of vegetation, making them inactive.

These distinct sites were chosen to provide natural microbiomes samples of higher microbial diversity given the different geographical origin and diverse ecosystems' characteristics.

1.2 Samples' processing and physical-chemical characterization

The seven collected samples were characterized for their physical-chemical characteristics, including pH, conductivity, total suspended solids (TSS), volatile suspended solids (VSS), and nutrients. Prior to the analyses, the soil samples were sieved to remove large fragments (Figure 2-A), while the root samples were milled with a kitchen blender (Figure 2-B). Both solid samples (~48 mL) were mixed with milli-Q water (to a total volume of 160 mL) to obtain suspensions with solids contents of approximately 30% (v/v). The sediments samples (Figure 2-C) were also mixed with milli-Q water to obtain suspensions of similar solids content.

The processed samples' pH was measured with an Orion star series ThermoScientific meter, while their conductivity was measured with a FiveEasy F20 conductometer.

The samples were centrifuged, and the solids-free supernatants were analysed for their contents in volatile fatty acids (VFAs) and sugars by high performance liquid chromatography (HPLC) using a Merck-Hitachi chromatographer equipped with an Aminex HPX-87H pre-column and a column from BioRad (USA). Sulphuric acid 0.01 M was used as the eluent at a flow rate of 0.6 mL/min and 50 °C operating temperature. VFAs were detected with a UV detector at a wavelength of 210 nm (Albuquerque et al., 2011), using acetate, propionate, butyrate, valerate and lactate (Merck, analytical grade) at

concentrations in the range 25–1000 mg/L as standards. Sugars were detected with a refractive index detector, using glucose, fructose, xylose and arabinose (Merck, analytical grade) as standards, at concentrations of 25–1000 mg/L.

Inductively Coupled Plasma-Atomic Emission Spectrometry (ICP-AES) was also conducted to quantify several elements in the solids-free supernatant samples. The analysis was performed in a Horiba Jobin-Yvon (Ultima, France), coupled with a 40.68 MHz RF generator (Czerny-Turner monochromator) with 1.00 m (sequential) autosampler AS500. For this analysis, the samples were acidified with one drop of nitric acid.

Figure 2: Processing of the collected samples: (A) soil samples; (B) plants root samples; (C) river sediments.

As shown in Table 1, The pH value of most samples was between 6.11 and 7.55. The exception was the soil from Buçaco Forest (Aveiro) that presented an acidic pH (4.02), considerably lower than the value (6.41) observed for the other soil sample collected at Mata dos Medos forest (Setúbal). Buçaco Forest soil also presented a lower conductivity (17.02 µS/cm), which agrees with the samples lower content in mineral elements (71.35 ppm) compared to Mata dos Medos soil sample (135.55 ppm) (Table 2). Low mineral elements' contents were also found for the fern and lima been roots, all collected at Aveiro region, which shows the collection site influences the samples' composition.

The sediment samples collected at the Tagus River mouth (Porto Brandão) and from the marshland (Corroios) presented the highest pH values 7.55 and 7.52, respectively (Table 1), together with significantly higher mineral elements contents (9306.93 and 8468.82 ppm, respectively) (Table 2). In both sediment samples, the most abundant elements were Na (6377 and 6322 ppm), Mg (1525 and 1436 ppm), K (869 and 399 ppm) and Ca (529 and 303

ppm). Sr (4.15 and 4.45 ppm) and B (2.36 and 1.84 ppm) were also detected for the two sediment samples, being absent in all the remaining. Those elements are among the most common minerals found in river sediments (Sakan et al., 2021).

Other elements, including Al, Fe, Mn, P, Si and Zn, were detected in some of the samples, but their concentrations were very low (<1 ppm) (Table 2).

Traces of VFAs (lactate, acetic and isobutyric acid) and sugars (glucose, fructose, xylose and arabinose) were detected in the solid-free supernatant of the some of the samples. Such compounds result from the microorganisms' activity, namely in the decomposition of organic material, such as lignocellulosic compounds.

Table 1: Natural microbiomes samples: origin and collection date, and the pH and conductivity values of the aqueous suspensions of the processed samples.

Type of sample	Sample origin	Collection date	pH	Conductivity (µS/cm)
Forest soil	Mata do Buçaco (Aveiro)	13/11/2021	4.02	17.04
	Mata dos Medos (Caparica, Setúbal)	05/11/2021	6.41	51.26
Sediment	Tagus River Mouth (Porto Brandão, Setúbal)	19/10/2021	7.55	45.31
	Tagus Estuarine Marshland (Corroios, Setúbal)	05/11/2021	7.52	36.63
Plant roots	*Carpobrotus edulis* (Beach dune plant, Caparica)	05/11/2021	6.89	85.69
	Dicksonia antartica (Fern, Mata do Buçaco, Aveiro)	13/11/2021	6.11	88.17
	Phaseolus lunatus (Lima Bean, home vegetable garden, Aveiro)	13/11/2021	7.07	51.17

Table 2: Elements detected in the solids-free supernatant of the processed natural microbiomes samples, by Atomic Emission Spectroscopy (ICP-AES).

Samples	Forest soil		River sediments		Plant roots		
Elements (ppm)	Mata do Buçaco	Mata dos Medos	Tagus Mouth	Marshland	Dune plant	Fern	Lima Bean
Al	0.07	0.18	0.14	0.26	0.06	0.56	0.25
B	N.D.	0.05	2.36	1.84	0.02	N.D.	N.D.
Ca	0.64	2.06	529	303	0.59	1.11	4.69
Fe	0.01	0.14	N.D.	0.01	0.13	0.05	0.14
K	57	68	869	399	84	53	65
Mg	0.5	1.5	1525	1436	3.1	0.8	2.8
Mn	N.D.	N.D.	N.D.	0.03	0.04	0.06	0.01
Na	13	61	6377	6322	67	12	13
P	N.D.	0.35	N.D.	0.58	1.45	0.03	1.08
Si	0.11	0.25	0.27	1.61	0.09	0.03	0.27
Sr	N.D.	N.D.	4.15	4.45	N.D.	N.D.	0.05

Zn	0.02	0.02	0.01	0.04	0.04	N.D.	0.04
Total	71.35	135.55	9306.93	8468.82	156.52	67.64	87.33

1.3 Samples' microbiological characterization

The general microbial composition of the environmental samples microbiomes was assessed by Fluorescence in Situ Hybridization (FISH), performed according to Amann (1995). The samples were fixed with 4% paraformaldehyde or ethanol (Nielsen et al., 2009). Aiming to characterize the bacteria present in each microbiome, several oligonucleotide probes were applied Fluorescein isothiocyanate (FITC)-labelled EUBmix probe for all Bacteria (mixture of EUB338 (Amann et al., 1990), EUB338-II and EUB338-III (Daims et al., 1999) and Cyanine 3 (Cy3)-labelled ALF969 for *Alphaproteobacteria* (Oehmen et al., 2006), BET42a for *Betaproteobacteria* and GAM42a for *Gammaproteobacteria* (Manz et al., 1992), Delta495a for *Deltaproteobacteria* (Loy et al., 2002), BAC303 for *Bacteroidaceae* and *Prevotellaceae* families, CF319a for most *Flavobacteria*, some *Bacteroidetes* and *Sphingobacteria* (Manz et al., 1996); LGC0354 for *Firmicutes* (Meier et al., 1999) and HGC69a for *Actinobacteria* (Roller et al., 1994). The oligonucleotide probes are specifically detailed in probeBase (Greuter et al., 2016). The slides were observed using an epifluorescence microscope, and the images were analyzed by Zeiss Imager D2 at 1000x.

FISH results shown the presence of major bacterial groups of *Proteobacteria*, *Firmicutes*, *Bacteroidetes*, *Actinobacteria* and *Cytophaga-flavobacteria* identified by the positive fluorescent signal of the oligonucleotide probes (Figure 3). No dominant bacteria group was observed within each microbiome, but some abundant populations were identified which is the case, for instance, of the *Gammaproteobacterial* population, targeted by the Cy3 labelled GAM42a probe, in the microbiomes collected from the river mouth sediments (Figure 3-C) and from Mata dos Medos soil (Figure 3-B), both collected in Caparica region. *Betaproteobacteria*, identified by the abundant positive signal of the BET42a probe, were observed in the microbiome of the dune plant roots *Carpobrotus edulis* (Figure 3-E).

	ALF969 Almost non-existent	LGC0354 Almost non-existent		
(A)	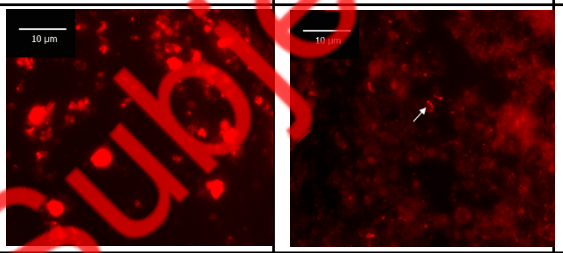			
	BET42 Present	GAM42a Abundant	HGC69a Almost non-existent	
(B)	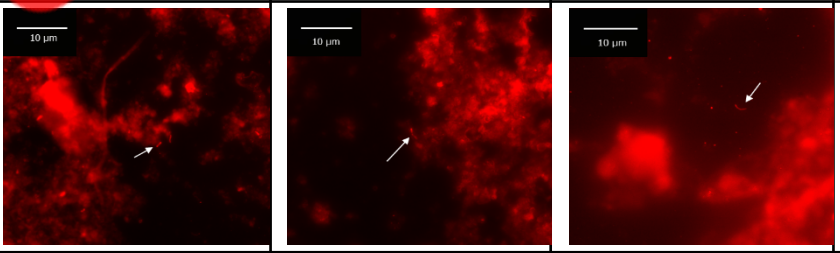			
	ALF969 Present	CF319 Present	DELTA495a Almost non-existent	GAM42a Abundant

(C)	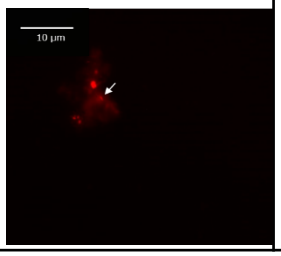	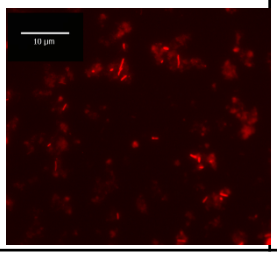	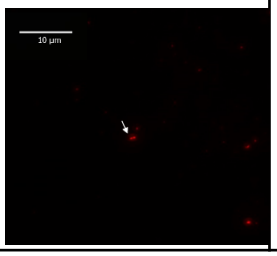	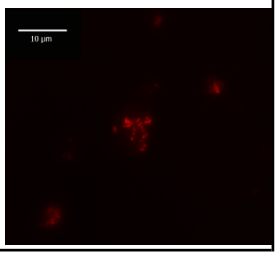

	BET42 Present	CF319a Almost non-existent	GAM42a Present	
(D)	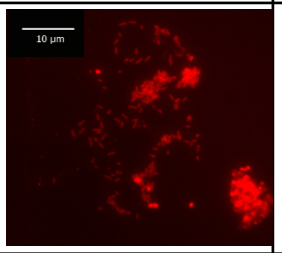	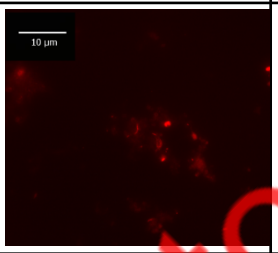	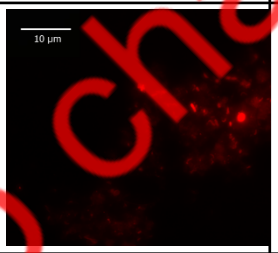	
	BET42 Abundant	DELTA495a Almost non-existent	GAM42a Present	
(E)	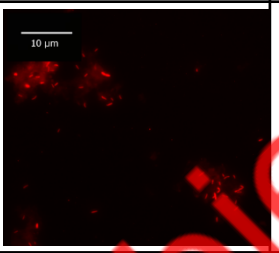	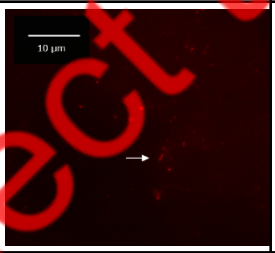	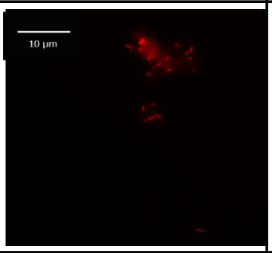	
	BET42 Present	DELTA495a Present	GAM42a Present	
(F)	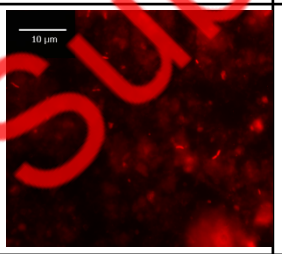	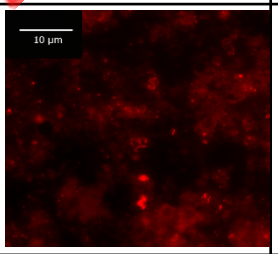	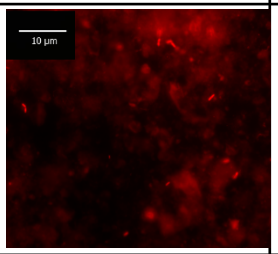	
	ALFA969 Present	BAC303 Almost non-existent	BET42 Present	CF319a Present
(G)	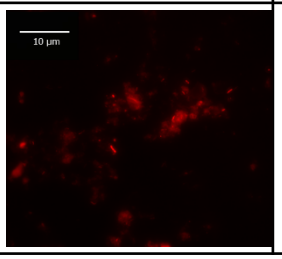	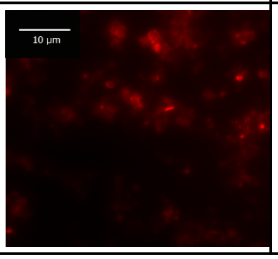	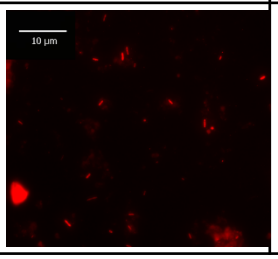	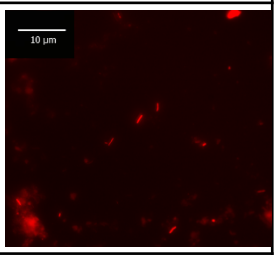

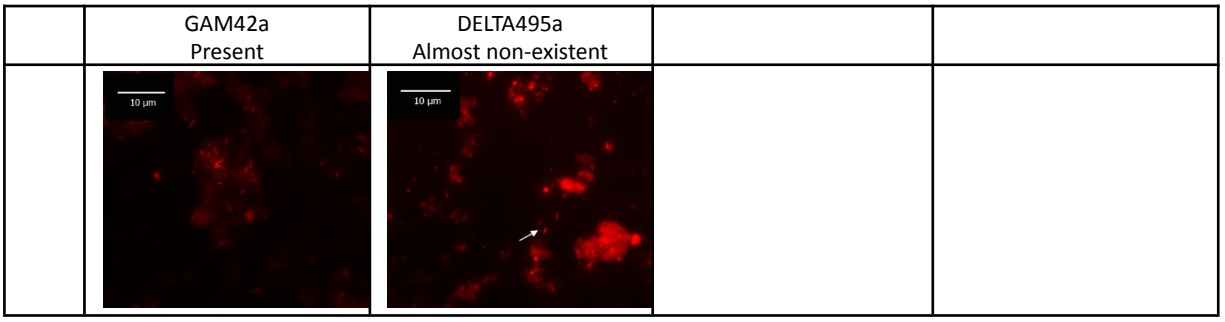

Figure 3: FISH images of the most abundant populations identified in environmental microbiome samples (1000x): (A) Mata do Buçaco forest soil; B) Mata dos Medos forest soil; C) river mouth sediments; D) marshland sediments; E) beach dune plant roots; F) Fern roots; G) Lima Bean roots. The images show bacteria hybridized with Cy3-labelled ALFA969 (red), BAC303 (red), BET42 (red), CF319a (red); DELTA495 (red); GAM42a (red); HGC69a (red) and LGC0355 (red). The scale bars for all panels are 10 µm. In the case of absence of bacteria in the different probes, the FISH images were not shown.

1.4 Heterotrophic Microbiomes Selection

1.4.1 Selection assays

Aiming to select for PHA-producing bacteria, a strategy of alternate feast-and-famine periods was imposed to each of the environmental microbiomes' samples. During the feast phase, the culture was fed with a suitable carbon source to promote cell growth, while during the subsequent famine phase the bacteria able to synthesize PHA will thrive, using the accumulated biopolymer as a source of carbon and energy. By imposing consecutive feast-and-famine cycles, a culture enriched in PHA-accumulating organisms is selected from the initial microbiome (Albuquerque et al. 2010).

The experiments (Figure 4) were performed in 500 mL baffled shake flasks with a working volume of 200 mL. The cultivation medium was composed of (per liter): anhydrous sodium acetate, 128 g; NH_4Cl, 16 g; $CaCl_2$, 0.7 g; EDTA, 1 g; $MgSO_4$, 6 g; KH_2PO_4, 2.25 g; K_2HPO_4, 9.24 g; Mineral solution, 1 mL. The mineral solution composition was as follows (per litre): $FeCl_3 \cdot 6H_2O$, 0.20 g; H_3BO_4, 0.32 g; $CuSO_4 \cdot 5H_2O$, 0.06 g: KI, 0.06 g; $MnCl_2 \cdot 4H_2O$, 0.26 g; $Na_2MoO_4 \cdot 2H_2O$, 0.13 g; $ZnSO_4 \cdot 7H_2O$, 0.26 g and $CoCl_2 \cdot 6H_2O$, 0.32 g. The pH value was adjusted to 7.0 before autoclaving. To each collected microbiome sample (160 mL), processed as described above (section 1.2), 40 mL of cultivation medium were added to give an initial acetate concentration of 20 g/L. Acetate was chosen as carbon source for the assays because it is a simple organic source commonly used for the production of PHA by mixed microbial consortia (MMC). Acetate eliminates the process of glycolysis, driving the metabolism towards carbon storage instead of the formation of intermediates of the β-oxidation pathway (Venkateswar Reddy et al., 2015). The shake flasks were incubated at 200 rpm and 20 °C. The assays had the duration of 10 days and were performed with two replicas (Figure 4).

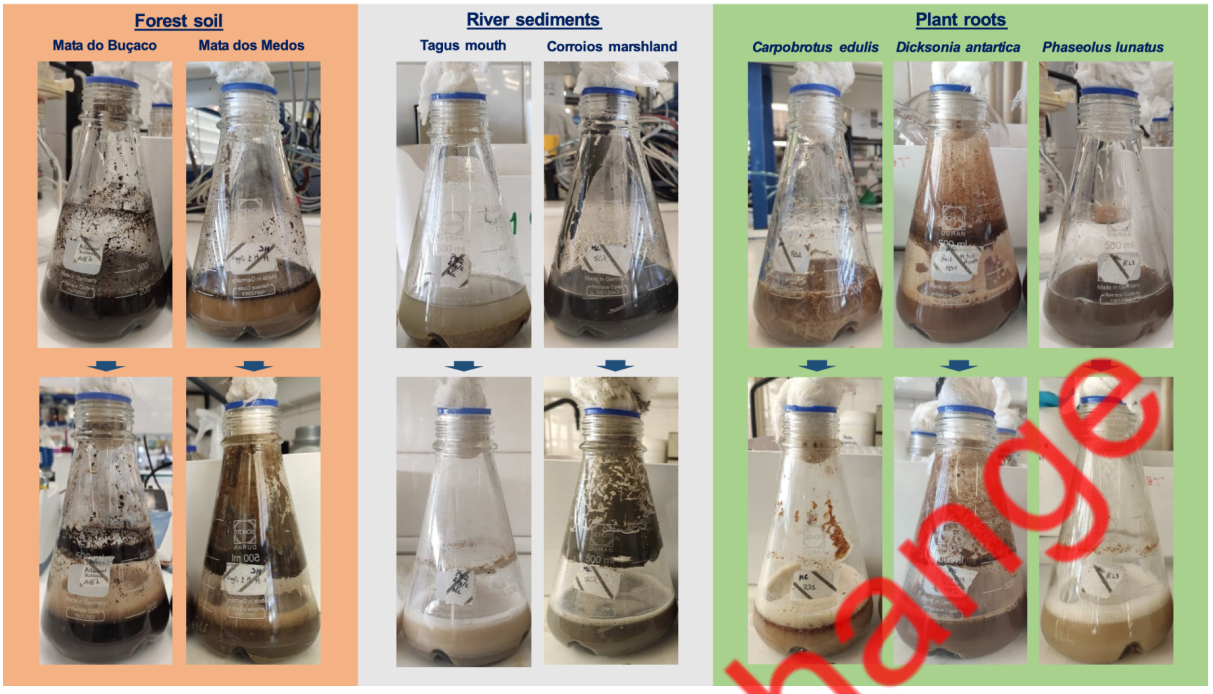

Figure 4: Shake flask assays for heterotrophic microbiomes' selection: Upper images: initial microbiome; Lower images: microbiome selected after 10 days with alternate feast-and-famine periods.

Samples (40 mL) were periodically (48-72 h) collected from each flask over the experiments, and replaced by the same volume of fresh medium, thus creating periods of alternate feast and famine conditions. At each sampling time, the pH was measured and adjusted to 7.0 ± 0.2 by the addition of 5 M NaOH or 5 M HCl. The culture broth samples were used for determination of the total suspended solids (TSS) and the volatile suspended solids (VSS), according to the Standard Methods (APHA, 1995). Briefly, 2-5 mL broth samples were filtered under vacuum with previously dried and weighed filters (Glass fibre filter, 0.45 µm, VWR). Then, the filters were dried at 105 °C until constant weight to determine the TSS. The samples were then incinerated at 550 °C for approximately 2 hours. The VSS was determined as the difference between the TSS and the ash weight obtained after incineration.

The supernatant obtained by centrifuging the broth samples (8000×g, 15 min, 4 ºC) was used for the quantification of acetate (by HPLC as described in section 1.2) and EPS (section 1.4.3). The resulting pellet was washed twice with deionized water, lyophilized and used for PHA quantification by gas chromatography (GC). The GC analysis was performed according to Cruz et al. (2016). Briefly, lyophilized samples (1 to 10 mg) were hydrolysed in 2 mL of methanol acidic (20%, v/v) sulphuric acid (SIGMA-ALDRICH) in methanol (Fisher Chemical) and 2 mL of benzoic acid in chloroform (1 g/L) (SIGMA-ALDRICH), on an oil bath at 100 ˚C, for 4 h. Then, 1 mL of deionized water was added. After phase separation, the organic phase, with the resulting methyl esters, was transferred to vials and analyzed by GC (430-GC, Bruker) with a Restek column of 60m, 0.53 mmID, 1 µM df, Crossbond, Stabilwax. The injection volume was 2.0 µL, with a running time of 32 min, a constant pressure of 14.50 psi and helium as carrier gas. The heating ramp was: 0 to 3 min, a rate of 20 ˚C/min, until 100 ˚C; 3 to 21 min, a rate of 3 ˚C/min, until 155 ˚C; and 21 to 32 min, a rate of 20 ˚C/min, until 220 ˚C. Hydroxybutyrate (HB) and hydroxyvalerate (HV) concentrations were determined through the use of two calibration curves, one for HB and other for HV, using

standards (0.1-10 g/L) of a commercial co-polymer P(HB-HV) (88%-12%) (Sigma), and corrected using heptadecane as internal standard (concentration of approximately 0.5 g/L).

1.4.2 Production of polyhydroxyalkanoates

Figure 5 shows the substrate (acetate) concentration for each feast-and-famine cycle, as well as the VSS and PHA content evolution, over the 10 days of the selection assays. The highest VSS increase was observed for the forest soil samples (Mata do Buçaco, 17.36 g/L, and Mata dos Medos, 18.46 g/L), and for the fern roots sample (17.66 g/L) (Table 3), for which the highest yield of VSS on a substrate basis were noticed (0.24-0.41 g_{VSS}/g_{Ac}).

It is noticeable that for all assays, except the lima bean microbiome sample (Figure 5-G), acetate uptake increased during the consecutive cycles (Figure 5-A, B, C, D, E and F). However, the specific substrate uptake rate first increased during the 1st/2nd cycles and then decreased (Table 3) for most assays. This result correlated with the fact that the VSS increased during the consecutive cycles.

During the 1st and 2nd cycles, acetate uptake was not complete, but on the 3rd or 4th cycles substrate exhaustion was observed for most assays. Such substrate depletion did not occur for the microbiomes selected from Mata dos Medos forest soil sample (Figure 5-B) nor the river mouth sediments sample (Figure 5-C). This shows that the feast-and-famine alternate conditions were not attained in all assays. Nevertheless, the accumulation of intracellular PHA granules was confirmed by visualization of the microbial cells by fluorescence microscopy (Olympus BX51) after Nile Blue staining (Figure 6). The cells stained with Nile Blue according to Silvestre et al. (2020). Briefly, a cell suspension in deionized water was mixed with Nile Blue A at a volume ratio of 1:10 (v/v) and treated at 50 °C for 10 min.

The PHA content in the microbiome was determined by GC analysis (Table 3). The highest PHA content (46.7 mg_{PHA}/g_{VSS}) was observed for the sediments' sample collected at the Tagus River marshland, which was attained after 5 days of cultivation, in the 2nd cycle (Figure 5-D). The decrease of the PHA content observed for the subsequent cycles can be explained by the fact that the samples were collected at the end of the cycles, when substrate exhaustion was experienced. Under such substrate limitation conditions (famine phase), the PHA-storing cells were able to thrive by utilizing their intracellular reserves, thus, the PHA content decreased. The same trend, lower PHA content for the cycles in which substrate exhaustion was attained, was displayed for Mata do Buçaco forest soil microbiome (Figure 5-A), and for the plant roots microbiomes (Figure 5-E, F and G).

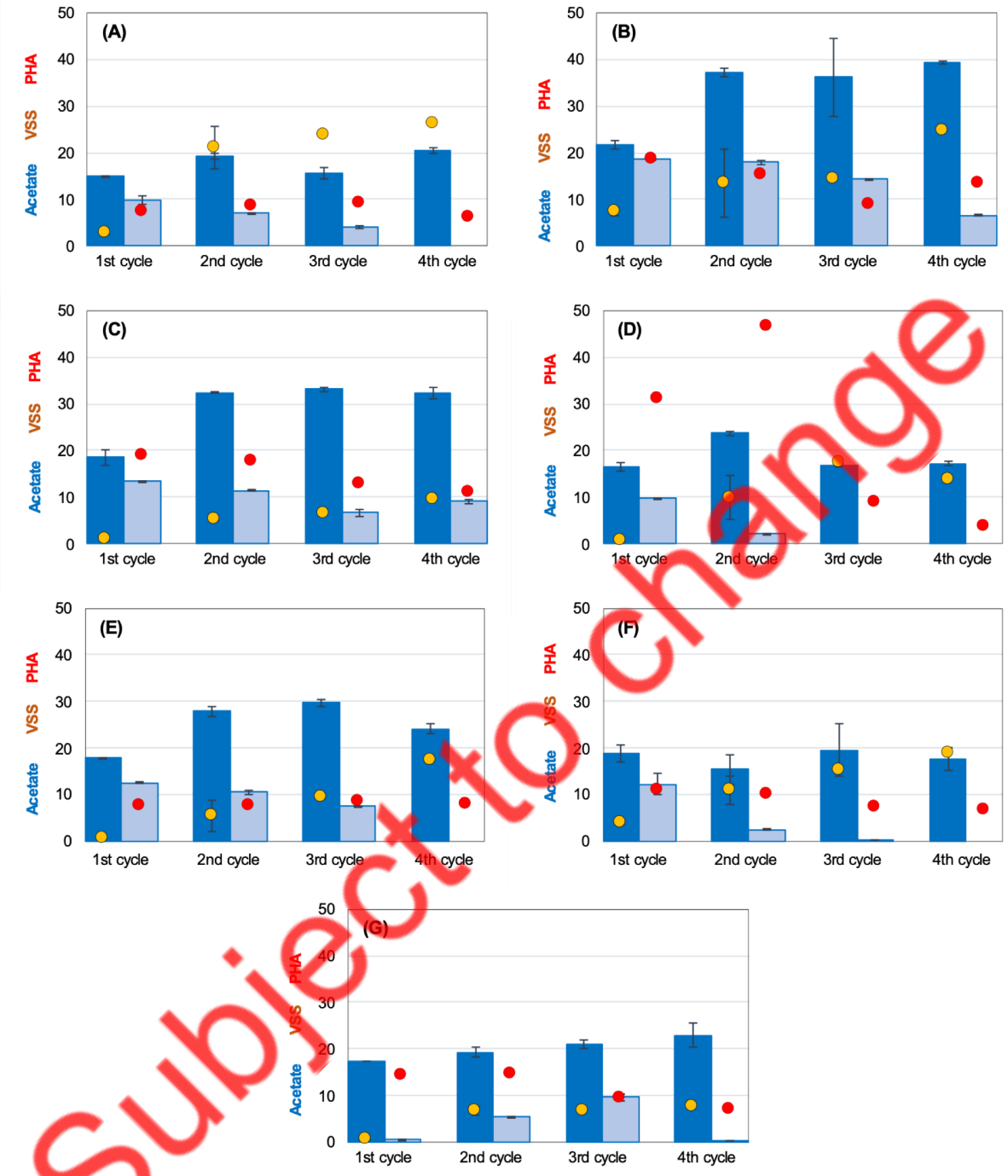

Figure 5: Results from the microbiomes' selections assays: Initial acetate concentration (g/L) (dark blue) and acetate concentration after each feast-and-famine cycle (light blue) (1st, 2nd, 3rd and 4th cycles correspond to days 3, 5, 7 and 10, respectively, of each assay); VSS (g/L; yellow circles) and PHA (mg_{PHA}/g_{VSS}; red circles). (A) Mata do Buçaco forest soil; B) Mata dos Medos forest soil; C) river mouth sediments; D) marshland sediments; E) beach dune plant roots; F) fern roots; G) lima bean roots.

Table 3: Main results obtained in the shake flask microbiome selection assays: TSS (g/L), VSS (g/L), overall acetate uptake (g/L), yield of VSS on a substrate basis $Y_{VSS/Ac}$

(g_{VSS}/g_{Ac}), specific acetate uptake rate for each feast-and-famine cycle ($g_{Ac}/(g_{VSS}.d)$); PHA_{max} (mg_{PHA}/g_{VSS}).

Microbiome	TSS (g/L)	VSS (g/L)	Overall Ac uptake (g/L)	$Y_{VSS/Ac}$ (g_{VSS}/g_{Ac})	Specific Ac uptake rate (gAc/(g_{VSS}.d))				PHA_{max} (mg_{PHA}/g_{VSS})
					1st cycle	2nd cycle	3rd cycle	4th cycle	*(day)*
Mata do Buçaco forest soil	29.62	17.36	49.46	0.35	0.080	0.260	0.219	0.337	9.2 *(7)*
Mata dos Medos forest soil	51.94	18.46	76.47	0.24	0.071	0.665	0.441	0.421	18.6 *(3)*
Tagus Mouth sediments	12.04	6.13	75.58	0.08	0.326	1.588	1.385	1.084	18.9 *(3)*
Marshland sediments	39.05	12.19	62.30	0.20	0.228	0.620	0.616	0.446	46.7 *(5)*
Dune plant roots	18.25	10.38	69.05	0.15	0.335	0.922	1.182	0.735	8.7 *(7)*
Fern roots	29.99	17.66	43.43	0.41	0.000	0.424	0.514	0.275	11.2 *(3)*
Lima bean roots	23.95	13.50	64.39	0.21	0.818	1.005	0.729	0.535	14.6 *(5)*

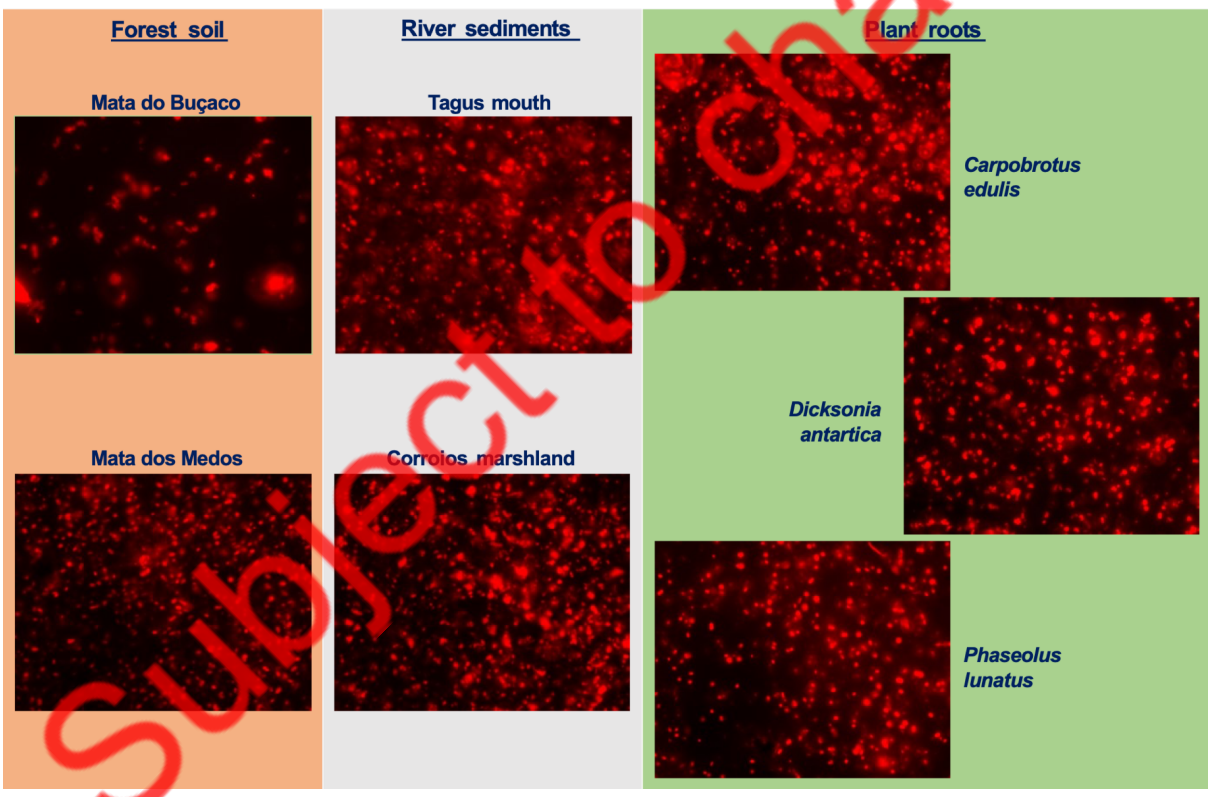

Figure 6: PHA granules visualization: Microbiomes' samples (collected after 10 days selection) were stained with Nile blue and observed using epifluorescence microscope, Olympus BX51, equipped with an Olympus XM10 camera (Cell-F software) under contrast phase and fluorescent light with a magnification of 1000x.

1.4.3 Production of extracellular polysaccharides

The EPS secreted by each microbiome during the 10 days selection assays were recovered from the supernatants by dialysis with a 12-14 kDa molecular weight exclusion membrane

(ZelluTrans Carl Roth - Regenerated Cellulose Tubular Membrane, Germany), against deionized water, at room temperature under constant agitation, with frequent water exchange over a period of 72 hours. The samples were then lyophilized, and the EPS was quantified by gravimetry. As shown in Figure 7, EPS production was noticed for all microbiomes. The biopolymers are materials of low density, with a cotton-like appearance. The EPS recovered from the microbiomes selected from the forest soil samples have a brownish coloration, while those selected from the plant roots are lighter, characterized by a pale beige color. The river sediments samples, on the other hand, are white.

Each tested microbiome yielded different EPS production (Table 4). The microbiomes selected from both forest soil samples produced considerable amounts of EPS (2.59 and 1.46 g/L, respectively). The beach dune plant roots selected microbiome also yielded a good EPS production (1.80 g/L), concomitant with the highest specific production among all tested microbiomes (164.0 mg_{EPS}/g_{VSS}). Interestingly, a high specific production was also noticed for the microbiome selected from the Tagus mouth sediments (134 mg_{EPS}/g_{VSS}), despite its low production (0.95 g/L).

Figure 7: EPS secreted by each microbiome after 10 days of cultivation in the selection assays: The biopolymers were recovered from the supernatant by dialysis and lyophilization.

Table 4: EPS production and sugar monomer composition for the shake flask microbiomes' selection assays (Man, mannose; Glc, glucose; Gal, galactose; Ara, arabinose; Fru, fructose; Fuc, fucose; GlcN, glucosamine; GlcA, glucuronic acid).

Microbiome	EPS production (g/L)	Specific EPS production (mg_{EPS}/g_{VSS})	Monosaccharides' relative molar ratio	Other unidentified constituents
Mata do Buçaco forest soil	1.46	72.1	Man : Glc : Gal 2 : 1 : 1	GlcN(?) + uronic acids
Mata dos Medos forest soil	2.59	100.0	Glc : Gal : Man : GlcA : Ara : Fru 3 : 3 : 2 : 2 : 1 : 1	GlcN(?) + uronic acids
Tagus Mouth sediments	0.95	134.0	Glc : Gal : Man : Ara 6 : 3 : 1 : 1	GlcN(?) + 2 unknown
Marshland sediments	0.77	59.9	Glc : Gal : Man : Fuc : Ara 3 : 2 : 2 : 2 : 1	GlcN(?) + 2 unknown + uronic acids
Dune plant roots	1.80	164.4	Glc : Gal : Man : Ara 3 : 3 : 1 : 1	GlcN(?) + 2 unknown + uronic acids
Fern roots	1.13	52.4	Gal : Ara : Man : Glc 6 : 3 : 2 : 1	GlcN(?) + uronic acids
Lima bean roots	0.82	58.0	Glc : Fuc : Gal : Man 4 : 2 : 1 : 1	GlcN(?) + 2 unknown + uronic acids

The EPS sugar monomer composition was determined by HPLC, following the biopolymers' hydrolysis with trifluoroacetic acid (TFA). For that, EPS dried samples (~5 mg) were dissolved in 5 mL deionized water and hydrolyzed with TFA (0.1 mL, 99%) at 120 °C, for 2 h. The hydrolysates were used for the identification and quantification of their constituent monosaccharides with a CarboPac PA10 column (Thermo ScientificTM DionexTM, Sunnyvale, CA, USA), equipped with an amperometric detector. Fucose, rhamnose, arabinose, galactose, glucose, fructose, ribose, glucuronic acid and galacturonic acid (Sigma-Aldrich) were used as standards (1 to 100 ppm). This analysis showed the heteropolysaccharide nature of the produced biopolymers (Table 4), whit glucose, galactose and mannose appearing as constituents of all EPS, while arabinose, fucose, fructose and glucuronic acid were detected in some of them. Other unidentified sugar monomers were noticed, including glucosamine and uronic acids other than glucuronic acid. The presence of some sugars, such as mannose, fucose or glucuronic acid, which are known to confer interesting biological properties to the polysaccharides (Roca et al., 2015), renders the EPS produced by the selected microbiomes of interest for further investigation to increase their production and to study their functional properties.

1.5 16s rRNA Characterization of the Heterotrophic Microbiomes

Fourteen heterotrophic microbiomes samples were analysed, including the initial environmental microbiomes (NovaIDi, where i=1, 3, 5, 7, 9, 11, 13) and the corresponding selected microbiomes (NovaIDii, where i=2, 4, 6, 8, 10, 12, 14), namely:

- NovaID1 and NovaID2: Tagus river mouth sediments;
- NovaID3 and NovaID4: Mata dos Medos forest soil;
- NovaID5 and NovaID6: beach dune plant roots;
- NovaID7 and NovaID8: river marshland sediments;
- NovaID9 and NovaID10 - Mata do Buçaco forest soil;
- NovaID11 and NovaID12: fern roots;
- NovaID13 and NovaID14 - lima bean roots.

DNA from the samples was isolated following QIAmt Power fecal Pro DNA Kit (Werfen), adding bead beating and enzymatic lysis steps prior to extraction to avoid bias in DNA purification toward misrepresentation of Gram-positive bacteria. A total of 50 ng of DNA was amplified following the 16S Metagenomic Sequencing Library Illumina 15044223 B protocol (ILLUMINA). In the first amplification step, primers were designed containing: 1) a universal linker sequence allowing amplicons for incorporation indexes and sequencing primers by Nextera XT Index kit (ILLUMINA); and 16S rRNA gene universal primers (Klindwoth et al., 2013). In the second and last assay, amplification indexes were included. 16S based libraries were quantified by fluorimetry using Quant-iT™ PicoGreen™ dsDNA Assay Kit (Thermofisher). Libraries were pooled prior to sequencing on the MiSeq platform (Illumina), 250 cycles paired reads con- figuration. The size and quantity of the pool were assessed on the Bioanalyzer 2100 (Agilent) and with the Library Quantification Kit for Illumina (Kapa Biosciences), respectively. PhiX Control library (v3) (Illumina) was combined with the amplicon library (expected at 20%).

Raw sequences, forward (R1) and reverse (R2), were imported into QIIME2 platform (Boylen et al., 2019). Cutadapt v3.4 (Marcel, 2011) plugin was used to filter specific V3-V4 16S region adapters. Raw samples were analyzed using Qiime2 platform, removing low-quality sequences with 'filterAndTrim' option. DADA2 software was used to denoise data and ASV were created. ASVs with less than five reads between all samples were removed to reduce background noise caused by sequencing errors. The taxonomic assignment of the ASVs was performed using two different methodologies and databases to obtain more precise annotation. The first assignation was made using BLASTN (Altschul et al., 1990) at the NCBI 16S ribosomal RNA database. The sequences which did not reach the 97% of homology with any of the database sequences were reassigned using the NBAYES algorithm (Bokulichet et al., 2018) on SILVA v.138 16S database. ASV with less than 10 counts in all samples were removed from the study. Data was normalized using rarefaction technique from Phyloseq R package (Weiss S et al., 2017) in order to perform alpha diversity analysis. Shannon, Simpson and Richness indexes were calculated using vegan R package (Oksanen J et al., 2019), and ANOVA test was used to find significant differences in alpha diversity between groups. The boxplots were by "vegan" and "stats," using R (v.3.3.1). The relative taxonomic abundances of the samples were displayed with histograms plotted by "microbiomeSeq" and "ggplot2" libraries in R (v.3.3.1).

After quality and chimeric sequence filtering, 624.148 reads were obtained (44.582 ± 5.988 per sample). The reads were grouped into 4715 bacterial amplicon sequence variants (ASVs). A rarefraction curve was calculated (alpha-diversity index) for all samples at the

ASV taxonomic level to evaluate the sequencing deep rightness. The samples reached the plateau area (Figure 8), so an increase in the number of sequences must not impact the number of ASVs detected.

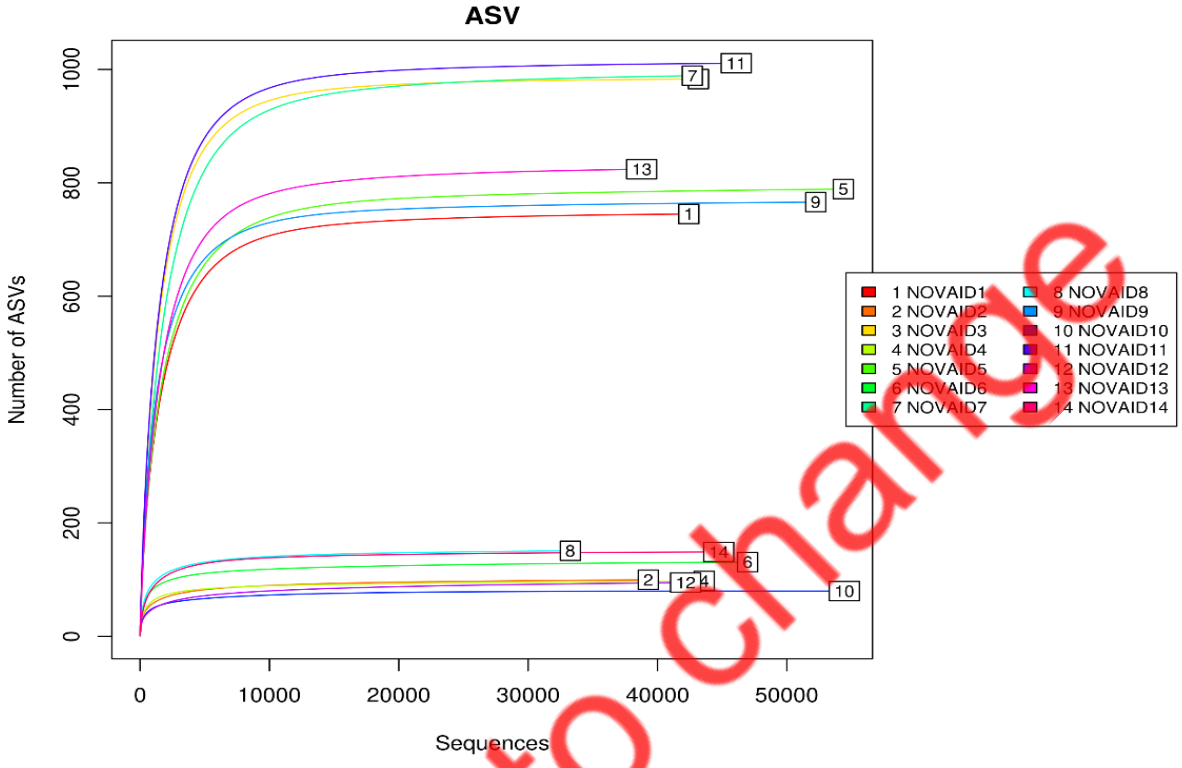

Figure 8: Rarefaction curves of bacterial population at ASV taxonomic level.

The 4715 ASVs belonged to 47 different phyla, being the most abundant phyla *Proteobacteria* (37.50 ± 12.75%), *Actinobacteria* (34.08 ± 15.47%), *Firmicutes* (10.57 ± 8.48%), and *Bacteroidetes* (3.55 ± 3.88%) (Figure 9). These results confirm those obtained by FISH (section 1.3) that also identified such bacterial groups. Comparing the initial environmental microbiomes (NovaID1, NovaID3, NovaID5, NovaID7, NovaID9, NovaID11 and NovaID13) to those of the corresponding selected microbiomes (NovaID2, NovaID4, NovaID6, NovaID8, NovaID10, NovaID12 and NovaID14, respectively), it is noticeable a considerable decrease of the microbial diversity of the samples. Moreover, there is a clear selection of *Actinobacteria*, whose relative abundance increased significantly for all selected microbiomes compared to the environmental samples. The microbiomes originating from soil samples (NovaID3 and NovaID9), despite their different geographical location (Caparica and Aveiro, respectively), had similar initial microbial composition, including members of the phyla *Acidobacteria* and *Verrucomicrobia*, for which no significant content was found in most of the other environmental samples, except for the plant roots of the fern (NovaID11) and of lima bean (NovaID13). Nevertheless, all these environmental samples evolved into similar selected microbiomes' composition, in which *Proteobacteria*, *Actinobacteria* and *Firmicutes* prevailed, and *Acidobacteria* and *Verrucomicrobia* were excluded.

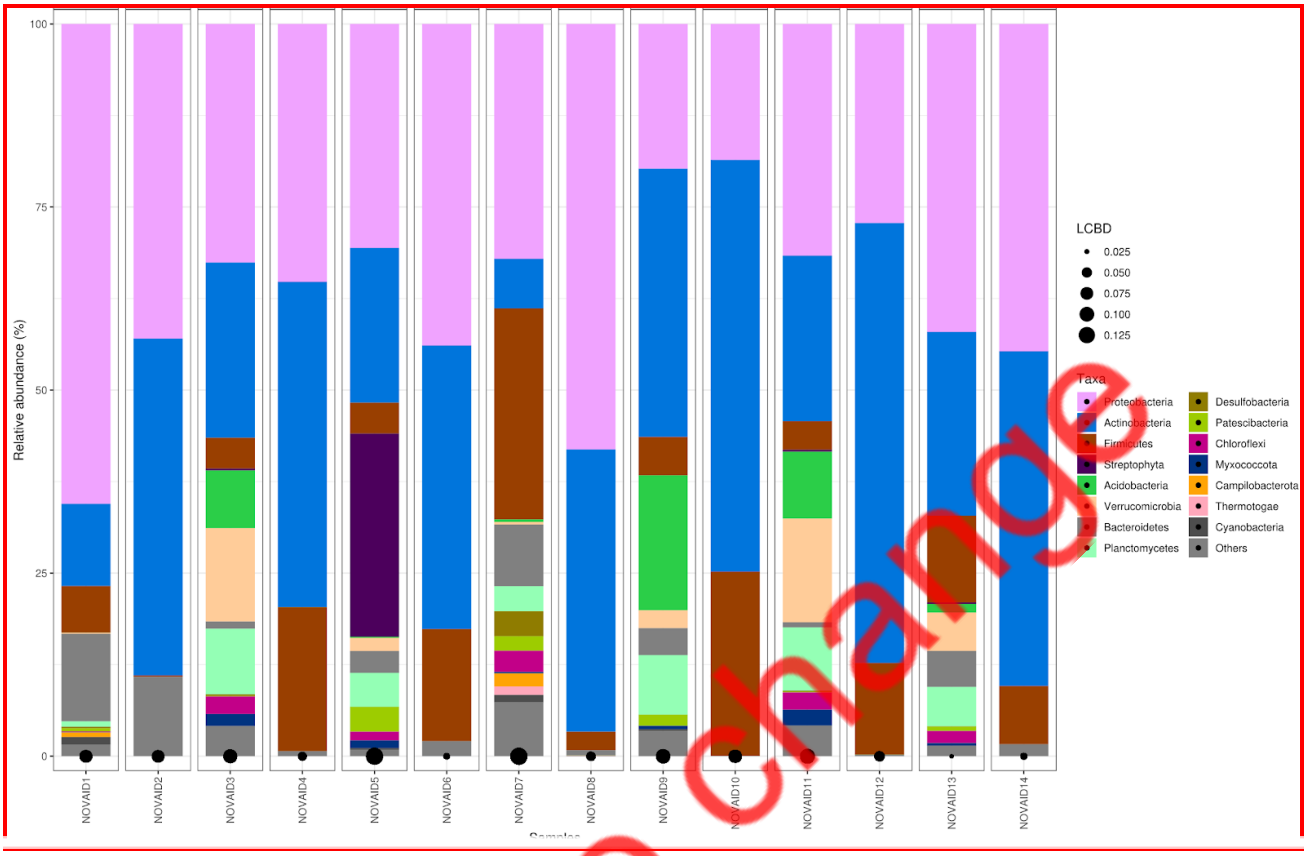

Figure 9: Relative abundances of the phyla and the LCBD values of all the samples. The label "others" represent the unknowns. NovaID1 and NovaID2: Tagus river mouth sediments, environmental and selected microbiomes; NovaID3 and NovaID4: Mata dos Medos forest soil, environmental and selected microbiomes; NovaID5 and NovaID6: beach dune plant roots, environmental and selected microbiome; NovaID7 and NovaID8: river marshland sediments, environmental and selected microbiomes; NovaID9 and NovaID10: Mata do Buçaco forest soil, environmental and selected microbiomes; NovaID11 and NovaID12: fern roots, environmental and selected microbiomes; NovaID13 and NovaID14: lima bean roots, environmental and selected microbiomes.

Families with the highest relative abundance across all the samples were *Corynebacteriaceae* (Phylum: *Actinobacteria*) (17.77 ± 17.67%), *Moraxellaceae* (Phylum: *Proteobacteria*) (11.60 ± 13.77%), and *Micrococcaceae* (Phylum: *Actinobacteria*) (7.67 ± 9.47%) (Figure 10), whose relative abundance clearly increased from the original environmental samples to the selected microbiomes after 10 days of cultivation under the feast-and-famine alternate cycles.

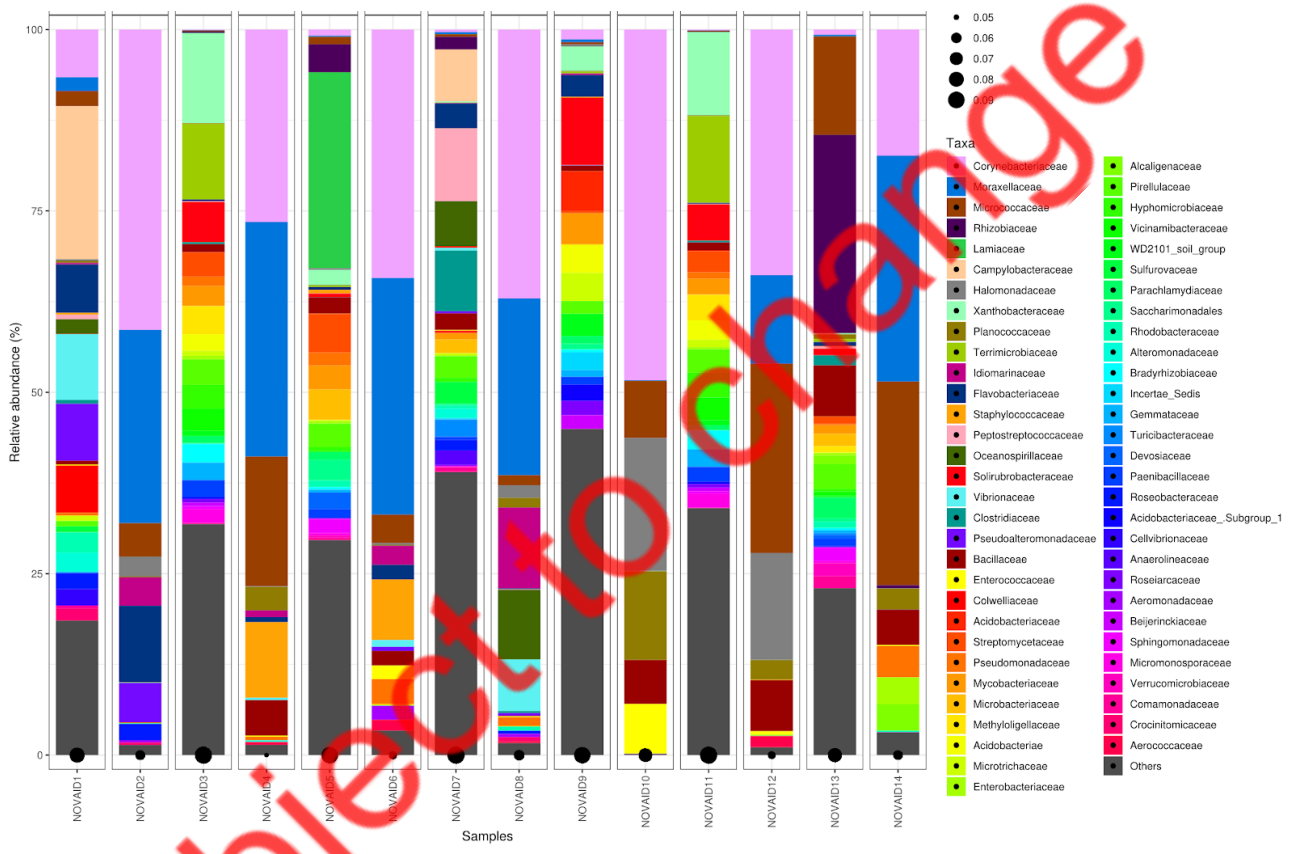

Figure 10: Relative abundances of the 62 most abundant families and the LCBD values of all the samples. The label "others" represent the unknowns. NovaID1 and NovaID2: Tagus river mouth sediments, environmental and selected microbiomes; NovaID3 and NovaID4: Mata dos Medos forest soil, environmental and selected microbiomes; NovaID5 and NovaID6: beach dune plant roots, environmental and selected microbiome; NovaID7 and NovaID8: river marshland sediments, environmental and selected microbiomes; NovaID9 and NovaID10: Mata do Buçaco forest soil, environmental and selected microbiomes; NovaID11 and NovaID12: fern roots, environmental and selected microbiomes; NovaID13 and NovaID14: lima bean roots, environmental and selected microbiomes.

A total of 483 genera were detected, of which the most abundant were: *Corynebacterium* (Phylum: Actinobacteria) (17.77 ±17.67%), *Psychrobacter* (Phylum: Proteobacteria) (8.13 ± 12.64%), and *Glutamicibacter* (Phylum: Actinomycetota) (3.74 ± 6.82%) (Figure 11).

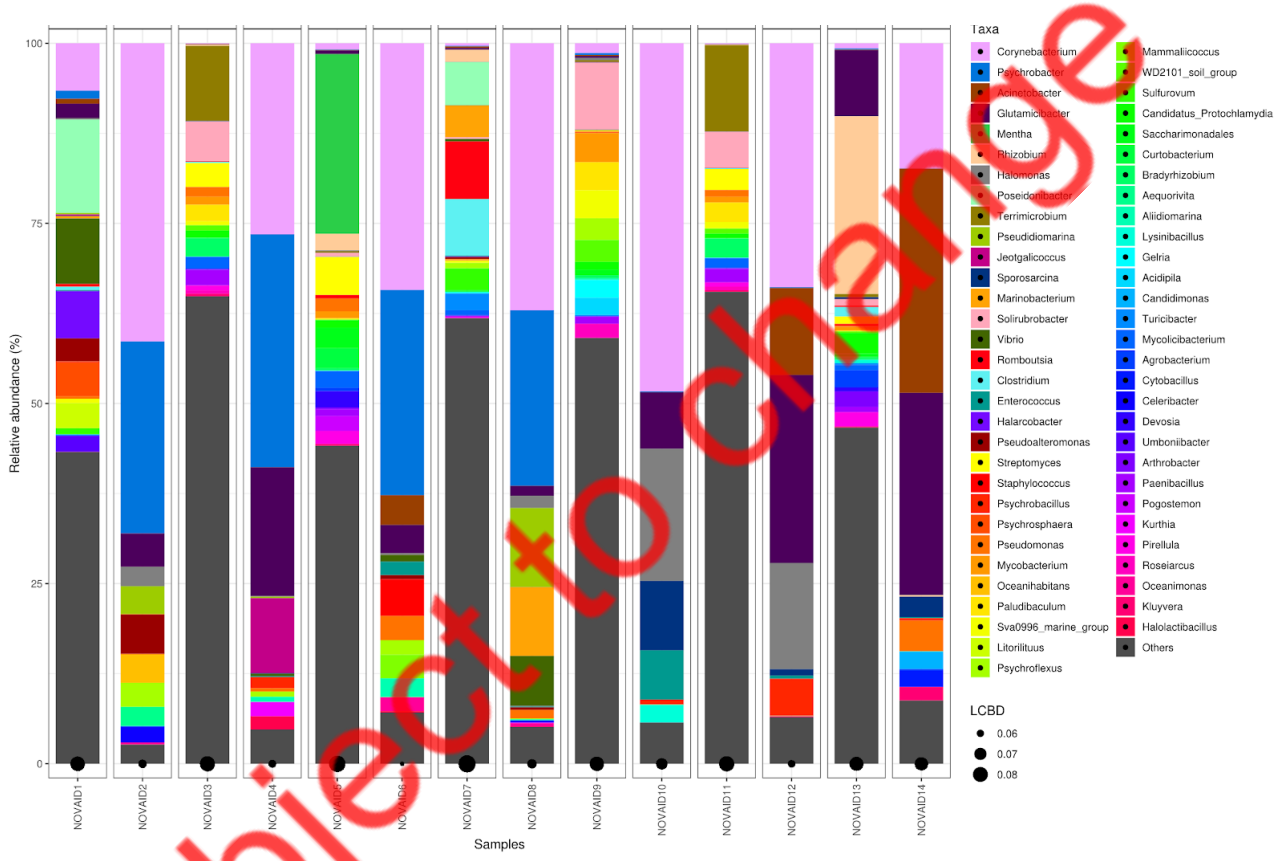

Figure 11: Relative abundances of the 62 most abundant genera and the LCBD values of all the samples. The label "others" represent the unknowns. NovaID1 and NovaID2: Tagus river mouth sediments, environmental and selected microbiomes; NovaID3 and NovaID4: Mata dos Medos forest soil, environmental and selected microbiomes; NovaID5 and NovaID6: beach dune plant roots, environmental and selected microbiome; NovaID7 and NovaID8: river marshland sediments, environmental and selected microbiomes; NovaID9 and NovaID10: Mata do Buçaco forest soil, environmental and selected microbiomes; NovaID11 and NovaID12: fern roots, environmental and selected microbiomes; NovaID13 and NovaID14: lima bean roots, environmental and selected microbiomes.

The samples originating from Setúbal area (NovaID1, NovaID3, NovaID5 and NovaID7) after the 10 days selection assays (NovaID2, NovaID4, NovaID6 and NovaID8) displayed a similar composition, with abundancy of members of the *Corynebacterium*, *Psychrobacter* and *Glutamicibacter* genera. On the other hand, the samples originating from Aveiro region,

although the initial environmental samples differed, also evolved towards predominancy of members of the *Corynebacterium* and *Glutacimibacter* genera. The microbiomes selected from root samples (NovaID6, NovaID12 and NovaID14) also revealed abundancy of *Acinetobacter* sp..

The genera *Corynebacterium* is widely distributed in nature, namely, in water, soil and plants, and it includes species with known ability to produce PHAs, such as, for example, *Corynebacterium glutamicum* (Ma et al., 2018). Such species was found in the microbiomes selected from the sediments of the Tagus River mouth (NovaID2 sample) and the Tagus marshland (NovaID8 sample), as well as from the soil collected at Mata do Buçaco forest (NovaID10 sample) (Figure 12). *Psychrobacter* sp., usually mainly found in sea water, deep sea and Antarctic Sea ice, include species isolated reported as PHA-producers (Tan et al., 2019) possessing also EPS production ability (Aullybux et al., 2019). The genus *Glutamicibacter*, which is ubiquitous in soil, water and air, was found in the samples from soil (NovaID 4) and roots (NovaID 12 and 14). This genus *Glutamicibacter* (previously *Arthrobacter* genus) include mostly salt or heavy metal tolerant rhizobacteria, with known EPS secreting ability. The microbiomes selected from soil and roots samples also revealed the presence of *Acinetobacter* sp., which may be found most in soil or plant samples and include PHA or EPS producers (Yadav et al., 2012; Zheng et al, 2021). *Halomonas* sp. (e.g., *Halomonas venusta*) were found in the selected microbiome from Mata do Buçaco forest soil and from the fern roots. Those species have also been reported as PHA and/or EPS producers (Stanley et al., 2018; Joulak et al., 2021).

The most abundant ASVs detected were: ASV2 [6] *Corynebacterium glutamicum* (4.78 ± 7.75%), ASV5 [6] *Psychrobacter fulvigenes* * 2 (3.14 ± 8.05), ASV3 [6] *Glutamicibacter protophormiae* (2.95 ± 4.79%), and ASV7 [6] *Glutamicibacter mysorens* * 2 (2.93 ± 6.55%) (Figure 11).

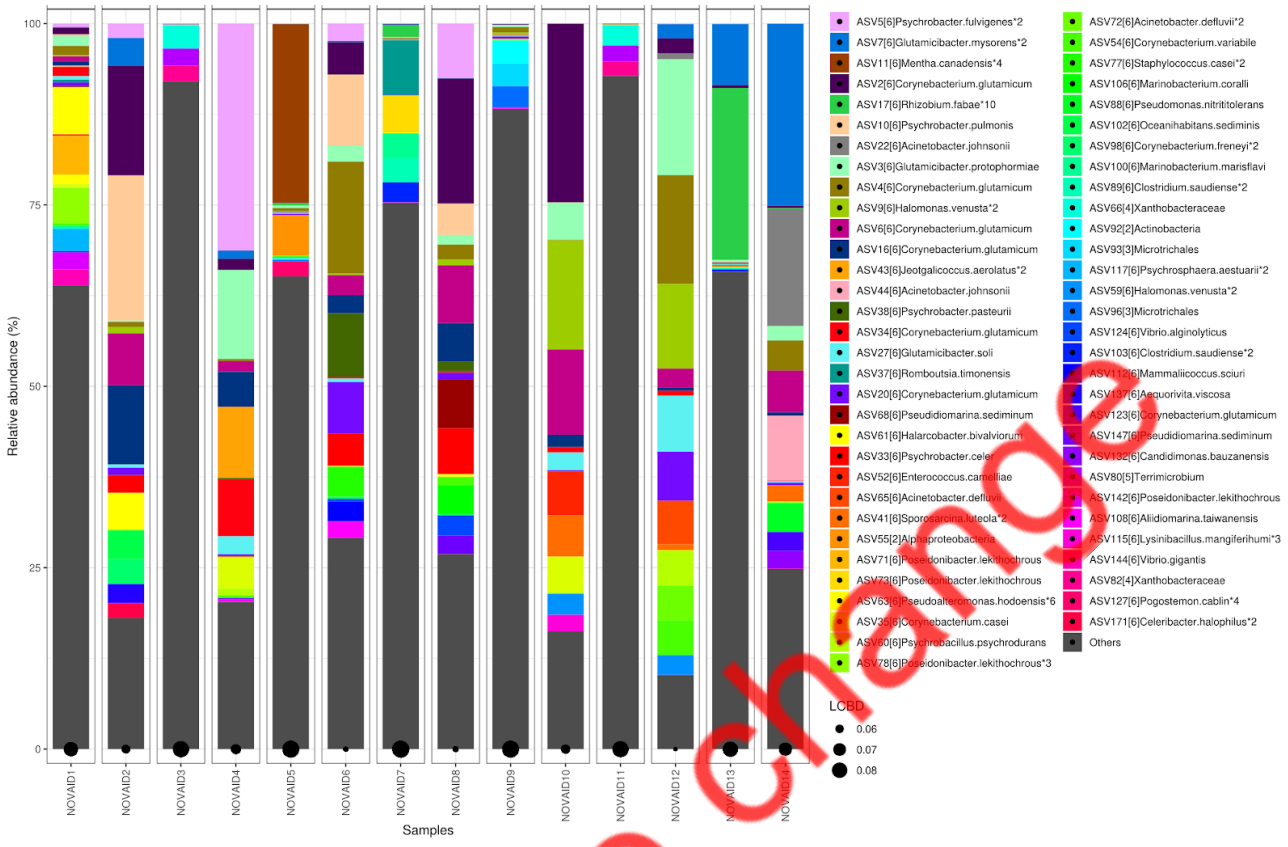

Figure 12: Relative abundances of the 62 most abundant ASVs and the LCBD values of all the samples. The label "others" represent the unknowns. NovaID1 and NovaID2: Tagus river mouth sediments, environmental and selected microbiomes; NovaID3 and NovaID4: Mata dos Medos forest soil, environmental and selected microbiomes; NovaID5 and NovaID6: beach dune plant roots, environmental and selected microbiome; NovaID7 and NovaID8: river marshland sediments, environmental and selected microbiomes; NovaID9 and NovaID10: Mata do Buçaco forest soil, environmental and selected microbiomes; NovaID11 and NovaID12: fern roots, environmental and selected microbiomes; NovaID13 and NovaID14: lima bean roots, environmental and selected microbiomes.

To analyze de alpha diversity Richness, Shannon and Simpson metrics, the metrics were significantly higher in time 0 group (T0) than time 10 group (T10) (Figure 13).

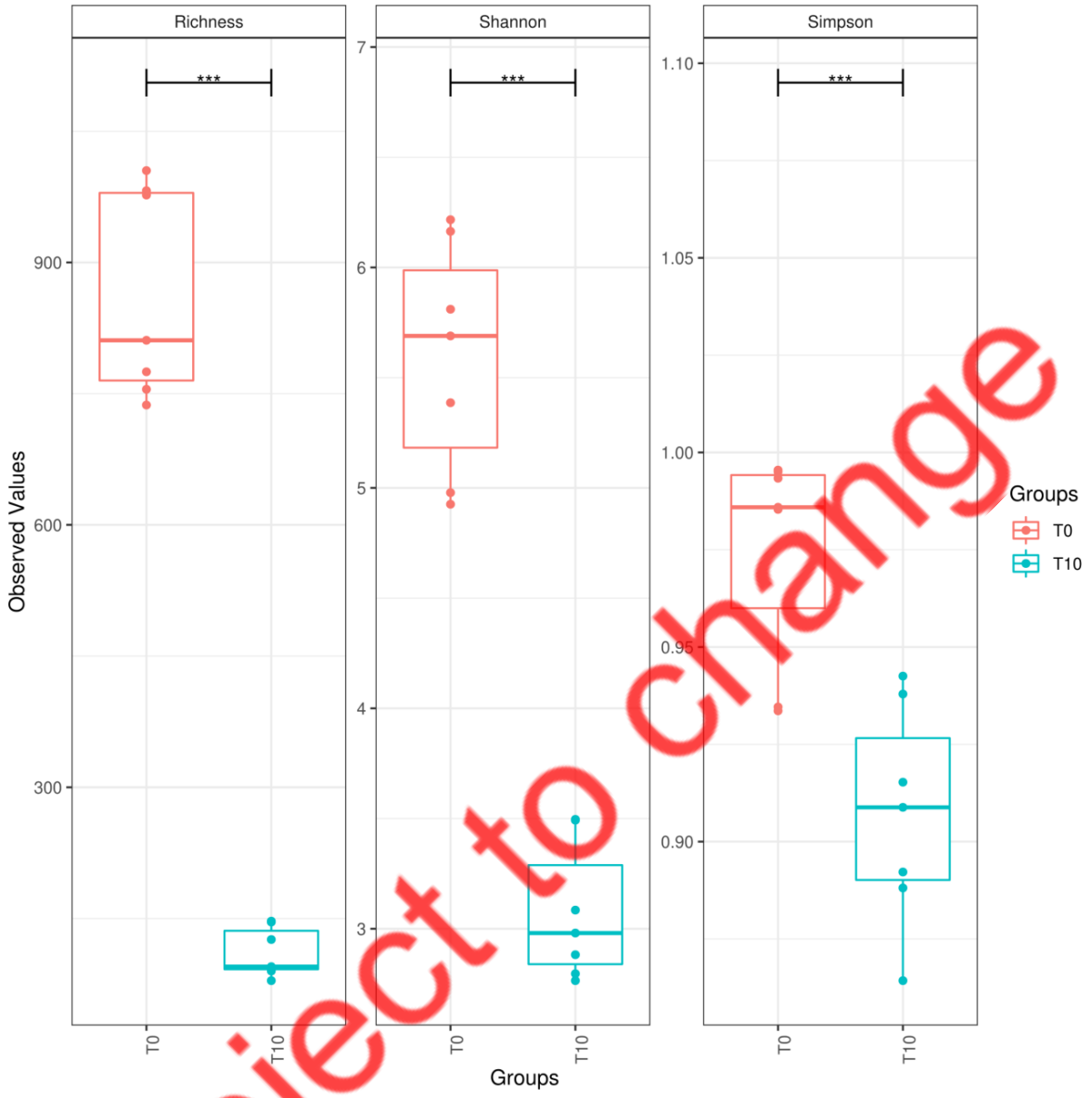

Figure 13: ASVs diversity of the bacterial microbiome of each group. Number of samples analyzed per group: Time 0:7 and Time 10:7. (*) indicate significant differences between groups according to ANOVA tests ($p < 0.05$).

2 Cyanobacteria Microbiomes

2.1 Environmental samples collection and site characterization

Environmental samples were collected from 4 different sites around Barcelona (Catalonia, Spain). Figure 14 shows the geographic location of the 4 sampling sites. To increase the genetic diversity of the collected samples, several sites with a variety of waters were selected: constructed wetland (CW), river (R), urban pond (UP) and a canal (C).

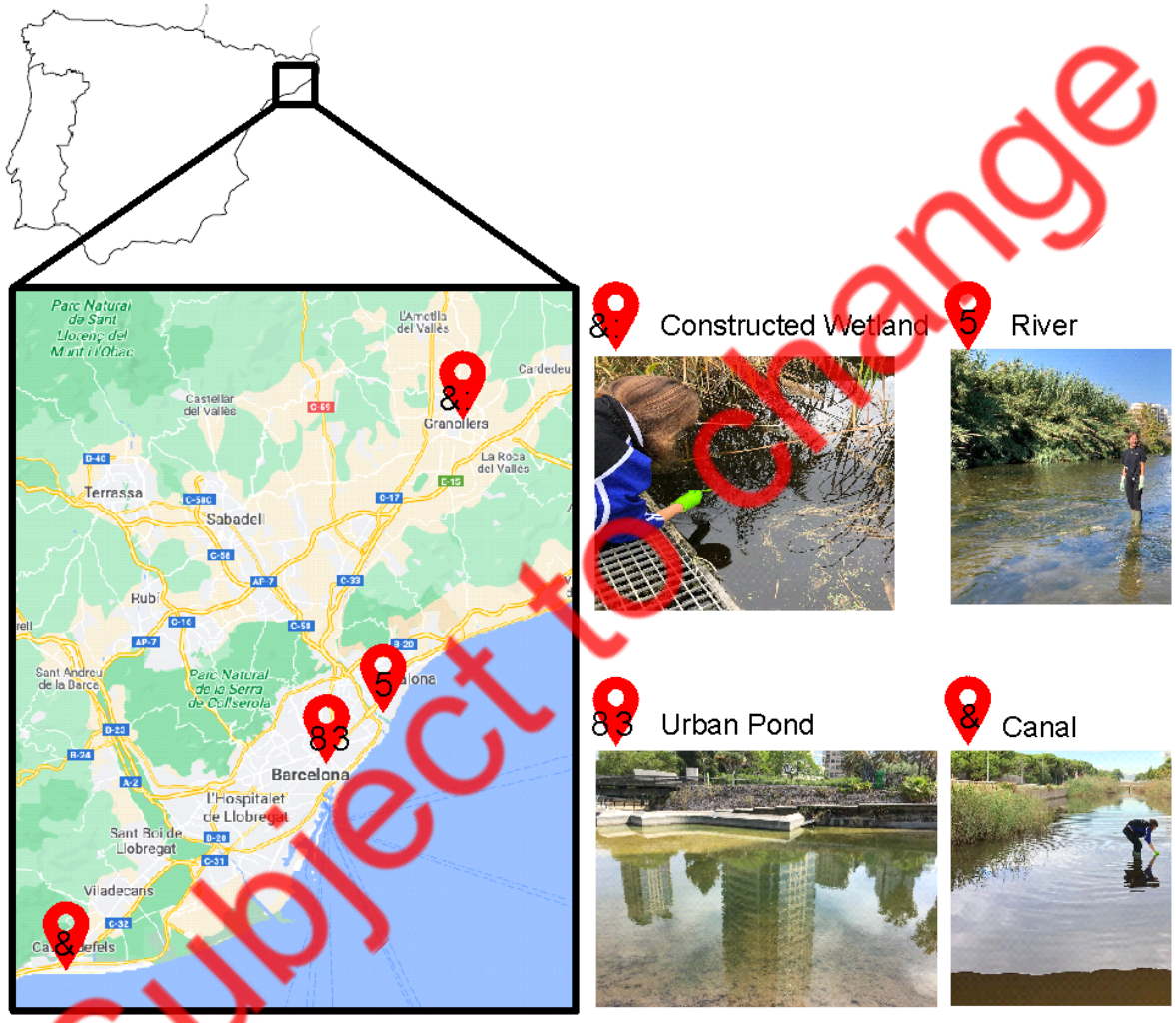

Figure 14: Geographic location of environmental samples for cyanobacteria microbiomes. Sites were selected along Catalonia geographic region (Spain). Red symbols in the left map represent the sampling sites. Pictures illustrate an image of the different sites during sampling.

The site of the constructed wetland (CW) in Can Cabanyes receives treated water from the wastewater treatment plant from the city of Granollers (secondary effluent). River (R) samples were collected from the Besòs river (Sant Adrià del Besòs). This an intermittent Mediterranean river which receives high amounts of treated wastewater discharged from the wastewater treatment plants in the metropolitan area of Barcelona. The urban pond (UP) is located in Diagonal Mar Park inside Barcelona city. The UP is fed with groundwater water. Canal (C) samples were taken from the Canal dels Canyars outlet, very near to the sea

(Gavà). This is a canal constructed in a natural deltaic creek to avoid flooding during storms in the surrounding built area.

The collection of the environmental samples involved the sampling of water and sediments for both microbiome development and site characterization. The results of the general physico-chemical characterization of the four collection sites, including pH, electrical conductivity, temperature, and nutrients, are shown in Table 5. $N\text{-}NO_3^-$ and $P\text{-}PO_4^{3-}$ were measured by the colorimetric methodologies 4500-NO3 and 4500-P, respectively, described in Standard Methods (APHA et al., 2012). Conductivity was measured using a conductometer (Conductometer GLP 31, Crison, Spain), and pH and temperature were measured by means of a pH probe (HI1001, HANNA instruments, Italy) and temperature probe (ABRA, Canada), respectively.

Table 5: Environmental samples general characterization.

Parameter	*Urban Pond*	*River*	*Canal*	*Constructed Wetland*
pH	8.04	8.03	7.04	7.6
Electrical Conductivity (mS/cm)	1.7	1.7	7.3	1.5
Temperature (°C)	26	23	20	20
Nitrogen (mg/L) ($N\text{-}NO_3^-$)	0	3.8	0.02	0
Phosphorus (mg/L) ($P\text{-}PO_4^{3-}$)	0	0.35	0	0
Collection date	1st June 2021	1st September 2021	15th November 2021	15th November 2021

The higher electrical conductivity in the canal could be explained due to its proximity to the sea. The river samples contained high nitrogen and phosphorus because of the influence of treated wastewater discharges. The urban pond and the constructed wetland had waters with low salinity in comparison to the canal, and with low nutrient concentrations in comparison to the river.

A total of 11 microbiome samples were collected from the four different sites. In detail, 4 samples were collected from the urban pond (labelled as UP 1–4), 2 from the canal (labelled as C 1–2), 2 from the constructed wetland (labelled as CW 1–2), and 3 from the river (labelled as R 1–3). In Table 6 information on the sampling origin for each sample and site is detailed.

Table 6: Detail of the collected samples for each site. (Wall and stone samples correspond to epilithic organisms; Water to planktonic; Sediment to benthic).

Urban Pond	*UP 1*	*UP 2*	*UP 3*	*UP 4*
Sample origin	Wall	Wall	Sediment	Sediment
Canal	**C 1**	**C 2**		
Sample origin	Sediment	Water		
Constructed Wetland	**CW 1**	**CW 2**		

Sample origin	Wall (outlet weir of the wetland)	Water	
River	**R 1**	**R 2**	**R 3**
Sample origin	Stone (near a sewer overflow)	Non-submerged sediment (near sewer overflow)	River stone

2.2 Environmental samples microbiome characterization

After microbiome sample collection, a first morphological characterization of the environmental samples was completed through microscopic observations under a bright light microscope (Motic, China) equipped with a camera (Fi2, Nikon, Japan) and a fluorescence microscope (Eclipse E200, Nikon, Japan) using the NIS-Element viewer® software. Figure 15 shows a general image of the most abundant microorganisms observed according to the different environmental sites and sample numbers.

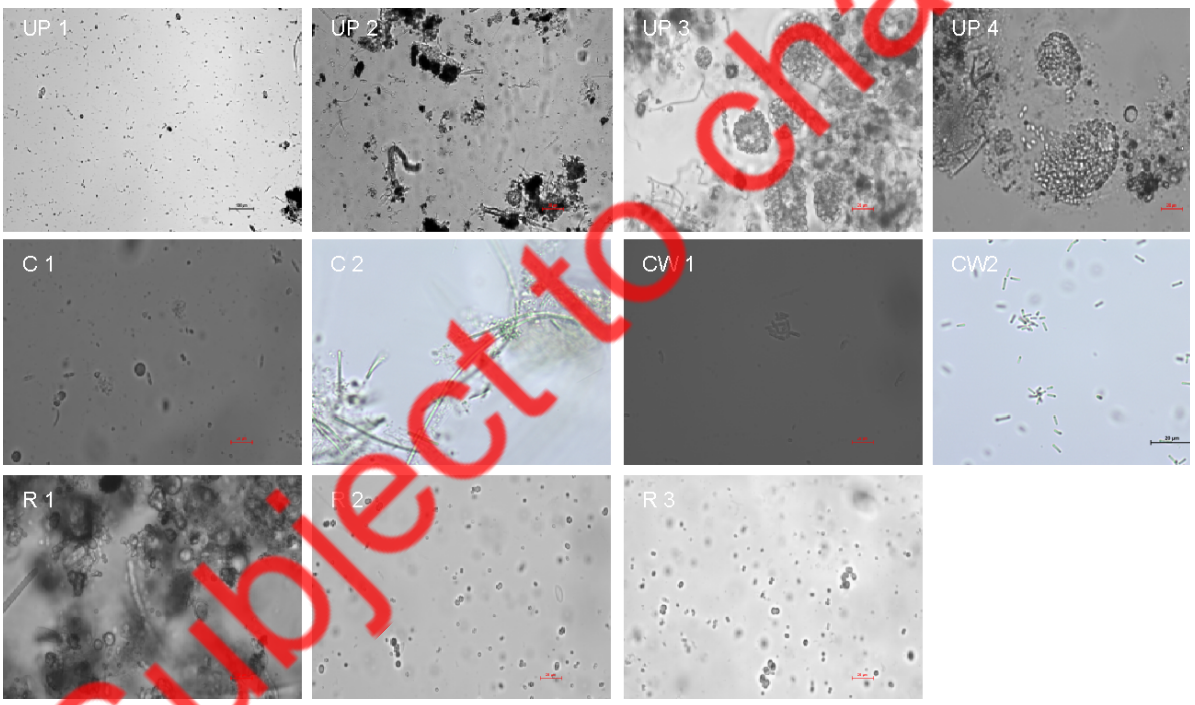

Figure 15: General Microscope images of the natural environmental microbiomes were observed under bright light microscopy at 200X and 400X. UP 1-4 correspond to environmental samples from Urban Pond. C 1-2 correspond to environmental samples from the Canal. CW 1-2 correspond to environmental samples from the constructed wetland. R 1-3 correspond to environmental samples from the Besós River. To see the images in more detail we suggest enlarging the photo on the computer screen. A very high diversity of microscopic organisms can be seen.

The natural environmental microbiomes consisted of mixed populations of cyanobacteria, eukaryotic microalgae (mostly green algae, diatoms) and other microorganisms such as euglenoids. Different taxonomic books and taxonomic references (Komárek and Hauer, 2013; Palmer et al., 1962; Streble and Krauter, 2018) were used to classify by morphology

the dominant species of green algae and cyanobacteria. Table 7 summarizes the most abundant organisms classified by microscopy observations.

Table 7: Environmental microbiome composition from microscopic images.

Sample	*Organisms*
UP 1	Diatoms; Cyanobacteria: *Synechocystis* sp. and filamentous Cyanobacteria; Green algae: *Cosmarium* sp.
UP 2	Cyanobacteria: *Synechocystis* sp.; Green algae *Cosmarium* sp.
UP 3	Cyanobacteria: *Aphanothece* sp.
UP 4	Cyanobacteria
C 1	Green algae: *Chlorella* sp., *Monoraphidium* sp., *Chlamydomonas* sp.
C 2	Filamentous and punctiform colonial Cyanobacteria
CW 1	Cyanobacteria: cf. *Gloeobacter* sp.
CW 2	Cyanobacteria: cf. *Gloeobacter* sp.
R 1	Filamentous cyanobacteria; Green algae: *Stigeoclonium* sp.
R 2	Cyanobacteria: *Synechocystis* sp.
R3	Cyanobacteria: *Synechocystis* sp.; Diatoms: *Cyclotella* sp., *Nitzschia* sp.; Euglenoids: *Euglena* sp.

Since the objective of task 2.1 was to develop cyanobacteria-rich microbiomes for the production of extracellular polysaccharides (EPS), polyhydroxyalkanoates (PHA) and phycobiliprotein pigments (PPP), we followed a selection strategy mostly based in phosphorus medium limitation (see Section 2.2.1). From our previous investigations, we know that cyanobacteria overcompete eukaryotic microalgae (in particular green algae) when the phosphorus concentrations are low (< 0.2 mg P/L) together with the application of N:P ratios between 7–22 (gram basis) (Arias et al., 2020). Note that we were particular concerned about the control of green algae because they are fast growers due to the higher affinity for these nutrients. On the other hand, it should be noted that the target bioproducts of the present project were not measured from raw environmental samples because of the low amount of biomass collected. Therefore, we analysed the bioproducts after growing the microbiomes in phosphorus limitation conditions (See section 2.2.1).

2.2.1 Cyanobacteria microbiome selection

Figure 16 describes the different cultivation phases applied to each microbiome sample since collection. The general purpose of the experimental set-up was to (i) select

cyanobacteria microorganisms (in particular among green algae) and (ii) obtain microbiome cultures with sufficient biomass concentration (i.e., approximately 1 $g \cdot L^{-1}$ VSS).

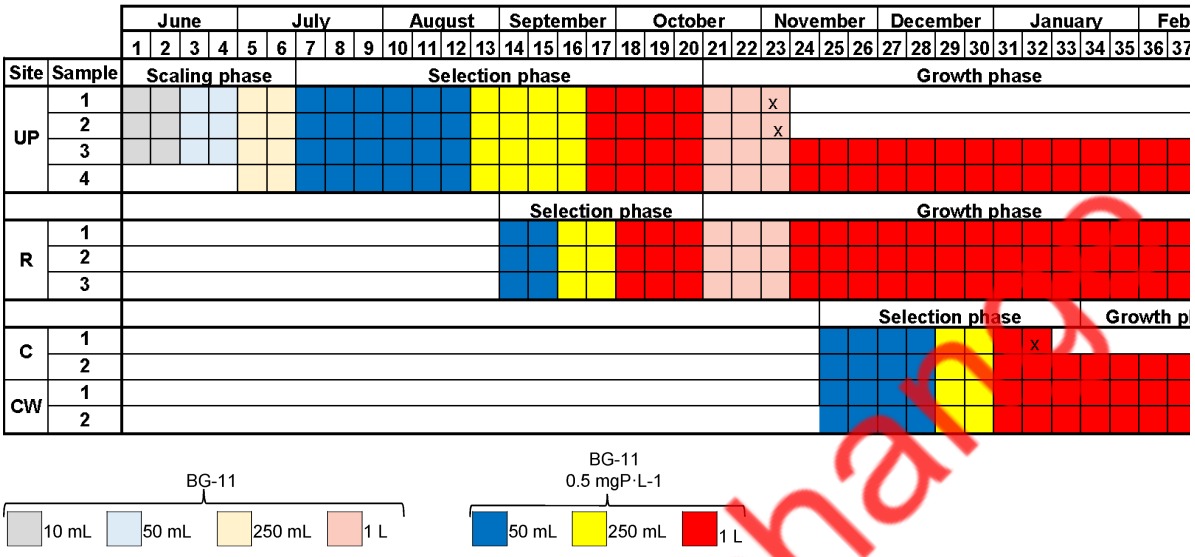

Figure 16: Graphical representation of the experimental setup for cyanobacteria microbiome selection. Colours represent the different media and culture volumes. Light colours represent BG-11 media, while dark colours indicate media with P limitation (a lower P concentration was applied instead of standard BG-11). Numbers under the months correspond to the weeks. Cross marks refer to removed samples.

Samples from the urban pond (UP 1-4) were collected in early June 2021. To start the cultures, 50 mL of samples were centrifuged, and the biomass was cultured in 10 mL test tubes with BG-11 medium (Figure 17a). Subsequently, the cultures were scaled up from 10 mL to 250 mL (Figure 17a-c) to essentially increase microbiome biomass. In general, we used visual observations such as changes in colour of the culture and microscope observations for this procedure. The scale-up ratio was of 1:5 to achieve proper cyanobacterial growth (Andersen, 2005).

Samples from the river (R 1-3) were collected in early September and samples from the canal (C 1-2) and constructed wetland (CW 1-2) in early November. Due to the experience previously gained from the urban pond samples, microbiomes were exposed directly to the selection phase by phosphorus limitation to get rid of green algae competition.

All samples were submitted to the selection phase consisting of a phosphorus nutrient limitation in BG-11 media (with low P content). Nutrient limitation was applied along with volume scale-up. In all samples, the selection procedure was effective to achieve microbiomes rich in cyanobacteria.

Following this period, the microbiomes were submitted to a growth phase in 1 L cultures: starting in mid-November in UP and R samples, and in mid-January from C and CW samples. Initially, microbiomes in the growth phase were cultured in BG-11 without any nutrient limitation. However, green algae overcompeted cyanobacteria in samples UP 2 UP 3 and C 1, which had to be discarded. As a result, and as a preventive measure, we decided

to maintain all the cultures with low phosphorus concentrations (0.5 mg·L^{-1}). In this growth phase, strict control of the physicochemical parameters was performed to increase microbiome biomass. Figure 18 show the temporal evolution of VSS during the month of January (i.e., growth phase) in samples UP 3,4 and R 1-2 and 3. Samples C 2, CW 1 and 2 started the growth phase in mid-January and data was not available at the time of writing this deliverable.

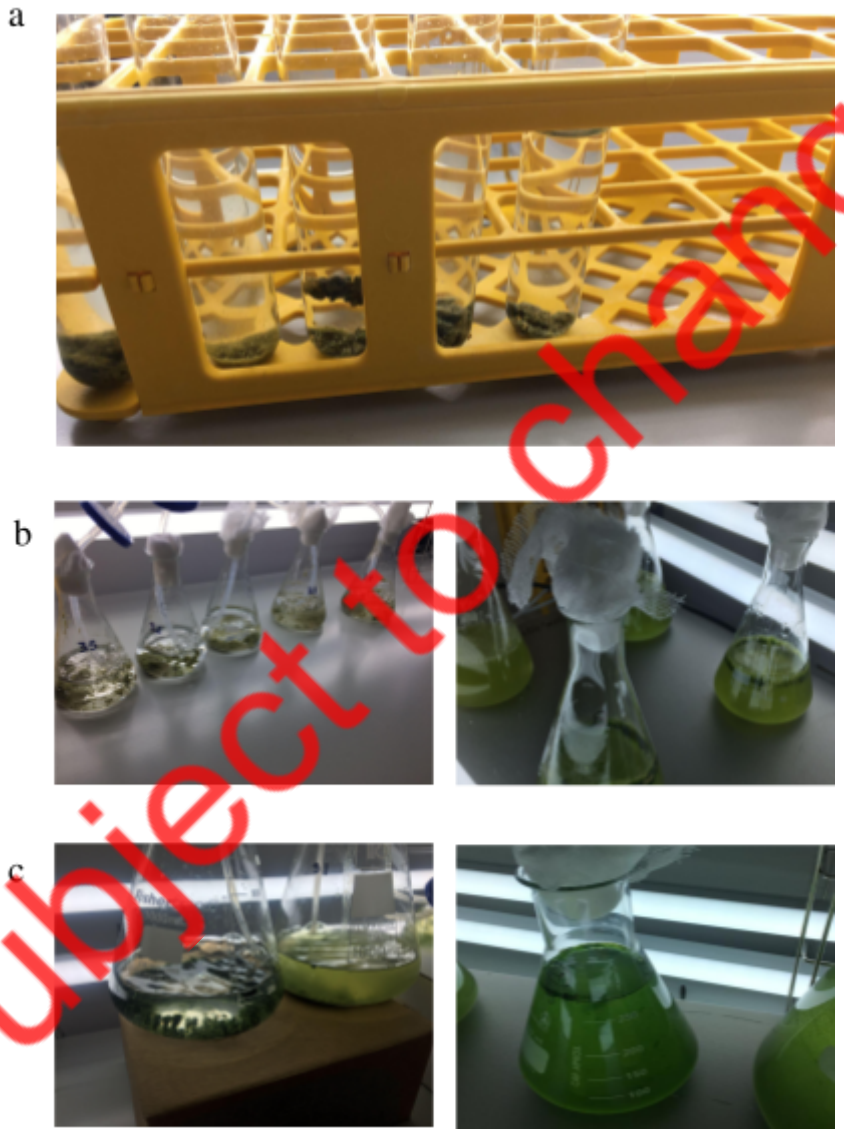

Figure 17: Images of microbiome scale-up phase in BG-11 media. a) 10 mL test tubes, b) 50 mL Erlenmeyer flasks and c) 250 mL Erlenmeyer flasks.

To keep the 1 L cultures continuously growing, approximately a third part of the volume (300 mL) was replaced every week by a new BG-11. These cultures were continuously agitated using magnetic stirrers. They were kept under 2.1 klx illumination under 15 h light: 9 h dark cycles at 30 ± 2 ºC. The pH was measured daily and kept at an optimum level (between 7.5 and 9) by daily injection of CO_2. Nitrogen (N-NO3) and phosphorus (P-PO4) were measured weekly and adjusted to a P of 0.5 mg·L^{-1} and N to 247 mg·L^{-1}. Note that N-NO3 is the only

source of N in BG-11. N-NO3 and P-PO4 were measured by the colorimetric methodologies 4500-NO3 and 4500-P, respectively, as described in the Standard Methods (APHA et al., 2012). Volatile suspended solids (VSS) were measured once per week following gravimetric method 2540-D described in Standard Methods (APHA et al., 2012). The microbiome was monitored using bright light microscopy and fluorescence microscopy.

To keep the 1 L cultures continuously growing, approximately a third part of the volume (300 mL) was replaced every week by a new BG-11. These cultures were continuously agitated using magnetic stirrers. They were kept under 2.1 klx illumination under 15 h light: 9 h dark cycles at 30 ± 2 ºC. The pH was measured daily and kept at an optimum level (between 7.5 and 9) by daily injection of CO_2. Nitrogen (N-NO3) and phosphorus (P-PO4) were measured weekly and adjusted to a P of 0.5 mg·L^{-1} and N to 247 mg·L^{-1}. Note that N-NO3 is the only source of N in BG-11. N-NO3 and P-PO4 were measured by the colorimetric methodologies 4500-NO3 and 4500-P, respectively, as described in the Standard Methods (APHA et al., 2012). Volatile suspended solids (VSS) were measured once per week following gravimetric method 2540-D described in Standard Methods (APHA et al., 2012). The microbiome was monitored using bright light microscopy and fluorescence microscopy.

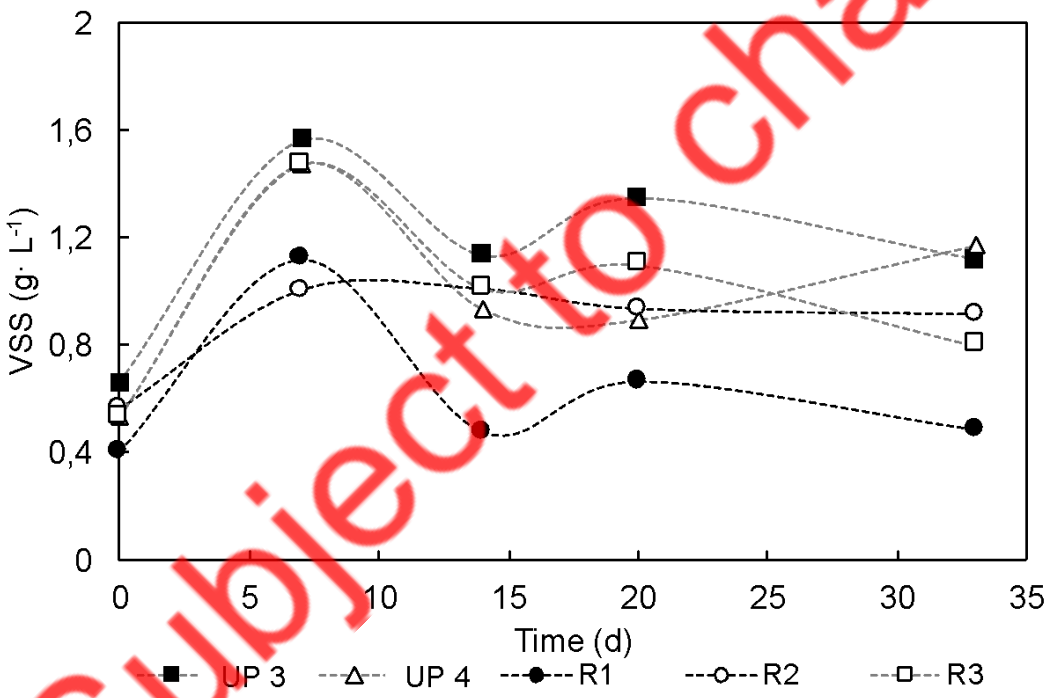

Figure 18: Volatile suspended solids (VSS) weekly follow-up for growth phase during January for samples UP 3, UP 4, and R 1-3.

2.3 Cyanobacteria microbiome characterization

Once cyanobacteria microbiomes were selected from the initial natural environmental samples, and the cultures were developed, we took samples from each culture in order to conduct i) microbiome characterization and ii) bioproduct characterization. Figure 19 shows microscope bright field images and fluorescence microscope images of the cyanobacteria

microbiomes which were characterized. The fluorescence microscope images reveal the magnificent predominance of cyanobacteria.

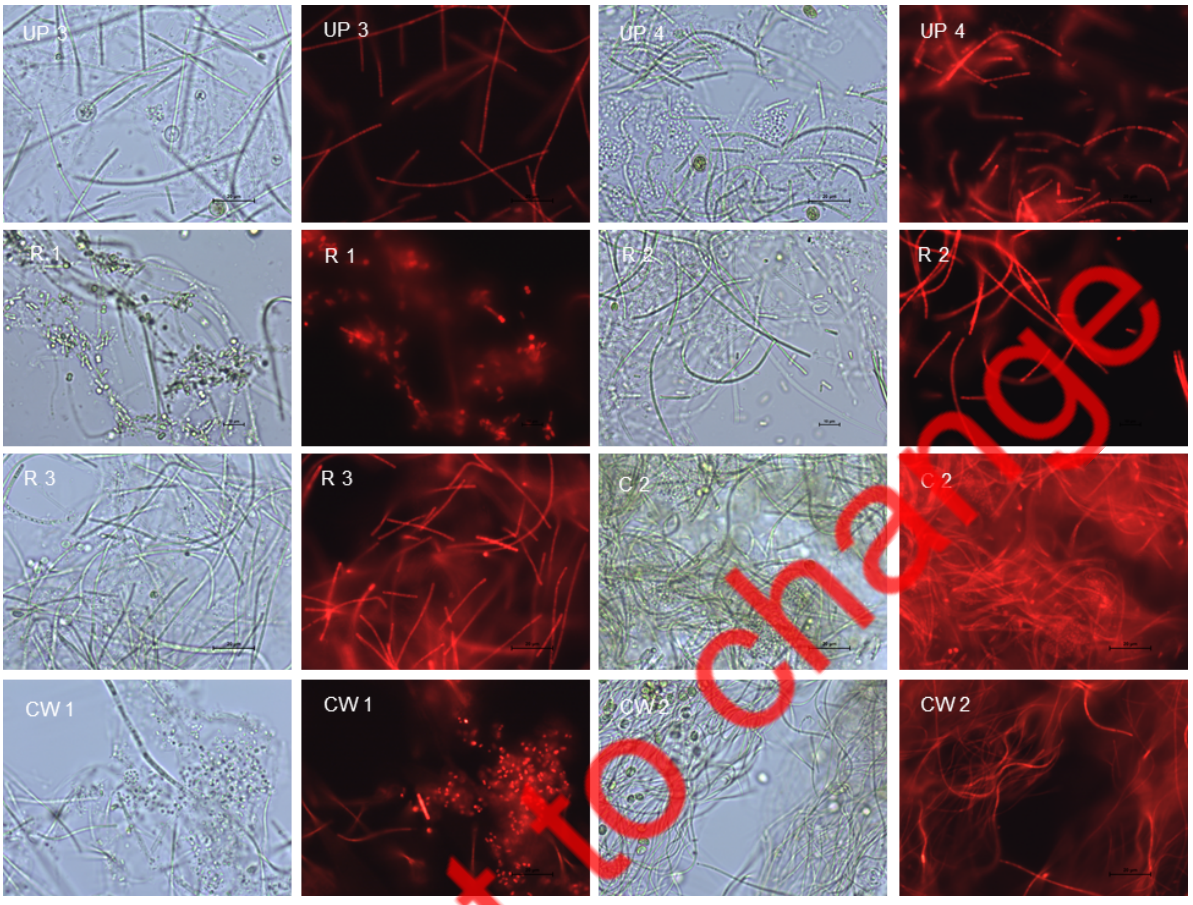

Figure 19: Microscope images of the grown cyanobacteria microbiomes observed under bright light and fluorescence microscopy at 400X. UP 1 and 4 correspond to samples from urban pond. CW 1-2 correspond to samples from the constructed wetland. C 2 correspond to the sample from the canal R 1-3 correspond to samples from the river.

Filamentous cyanobacteria and green algae are observed in UP 3 and UP 4 samples. In river samples: R 1 filamentous cyanobacteria and *Synechocystis* sp., R 2 filamentous cyanobacteria and cf. *Gloeobacter* sp and R 3 filamentous and punctiform colonial cyanobacteria. In canal sample C 2 filamentous and punctiform colonial cyanobacteria. In constructed samples CW 1 filamentous and punctiform colonial cyanobacteria and CW 2 filamentous and punctiform colonial cyanobacteria and cf. *Gloeobacter* sp.

2.4 Cyanobacteria bioproduct characterization

The analysis of the bioproducts was conducted from the scaled-up samples described previously. More specifically, samples for bioproducts were taken out during the growth phase at the end of January (Figure 16).

2.4.1 Polyhydroxyalkanoates (PHA)

PHB extraction and analysis were adapted from the methodology described by Lanham et al. (2013). Briefly, 1 mL of MeOH acidified with H_2SO_4 (20% v/v) and 1 mL of $CHCl_3$ containing benzoic acid as internal standard was added to 2–3 mg of lyophilized biomass located in assay tubes. Tubes were then incubated in a dry-heat thermo-block (Selecta, Spain) for 5 h at 100 ºC. After that, they were rapidly cooled on ice for 30 min, and 0.5 mL of deionized water were added to each tube. After, they were vortexed for 1 min to separate the different solvents by density. $CHCl_3$ was removed with a Pasteur pipette and placed into a vial with molecular sieves to remove the water that could remain in the sample. PHB was determined by means of gas chromatography (GC) (7820A, Agilent Technologies, USA). It was quantified by measuring the PHB monomers hydroxybutyrate (HB) and hydroxyvalerate (HV), using the co-polymer of PHB-PHV as a standard for HB and HV. A calibration curve with six points was prepared and processed in the same way as the samples. The results of PHA are shown in Table 8 expressed as a percentage of dry weight.

Table 8: PHA concentration of the different cyanobacteria microbiomes.

Sample	UP 3	UP 4	R 1	R 2	R 3	C 2	CW 1	CW 2
PHA ($\%_{dcw}$)	1.2	1.9	0.4	0.2	2	1.2	1.7	1.7

As expected, the amount of PHA was low in all samples without any clear trend related to the sampling site and PHA content. Samples with the higher content were R 3 and UP 4, whereas those with lower content were R 1 and R 2. Interestingly, the microscopic observation of samples with major PHA content (i.e., R 3 and UP 4) showed a major content of filamentous and punctiform colonial cyanobacteria.

2.4.2 Phycobiliprotein pigments (PPP)

For the extraction of phycobiliproteins, the procedures reported by Arashiro et al., (2020) and Zavřel et al. (2018) were combined and adapted to the conditions of this study. Freeze-dried biomass (~ 3 mg) was used to extract phycobiliproteins. Biomass was distributed in 1.5 mL tubes, and 1 mL of phosphate buffer (pH 7, 0.1 M) was added to each sample. Firstly, a preliminary freeze-thaw cycle (-21°C to 4°C) was performed. Then, glass beads (0.3 g of ø 0.1 mm beads, and 6 units of ø 2 mm beads) were added in each tube to disrupt cells by bead beating (3200 rpm, 10 min) at 4ºC using a vortex (Vortex-Genie™ 2, Scientific Industries SI™). Finally, the disrupted samples were centrifuged (9500 xg, 25ºC) for 15 min, and the supernatants were collected and measured in a plate reader (Synergy™ HT, BioTek) at OD_562nm, OD_615nm and OD_652nm, which are the wavelengths that correspond to the maximum absorption of phycoerythrin (PE), phycocyanin (PC), and allophycocyanin (APC), respectively. Phosphate buffer was used as a blank. The concentrations of were quantified according to Bennett and Bogorad (1973):

- PC (mg/L) = [OD_615nm- (0.474*OD_652nm)]/5.43
- APC (mg/L) = [OD_652nm- (0.208*OD_615nm)]/5.09
- PE (mg/L) = [OD_562nm- (2.41*PC) – (0.849*APC)]/9.62

All the analyses were performed in triplicates and under dark conditions to avoid pigment degradation. The results of the of PPP are shown in Figure 20.

D

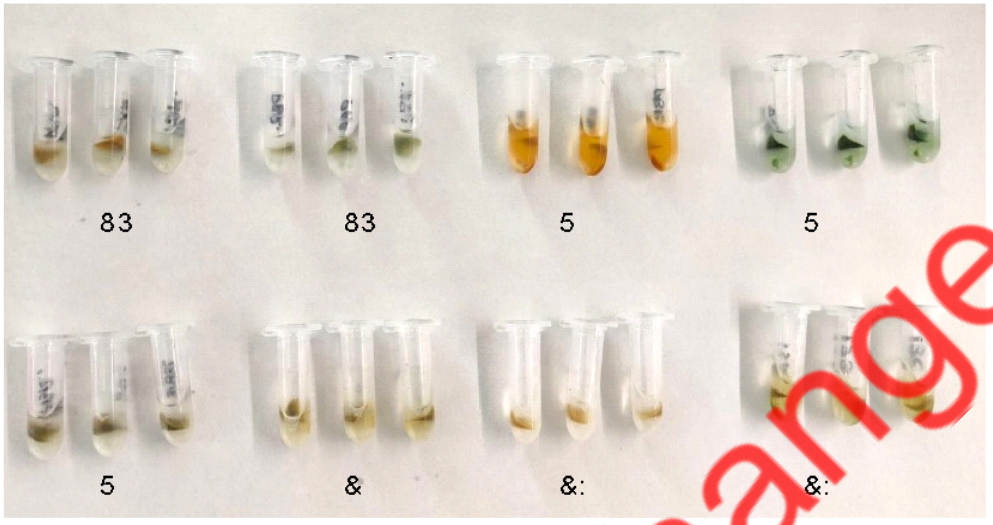

E

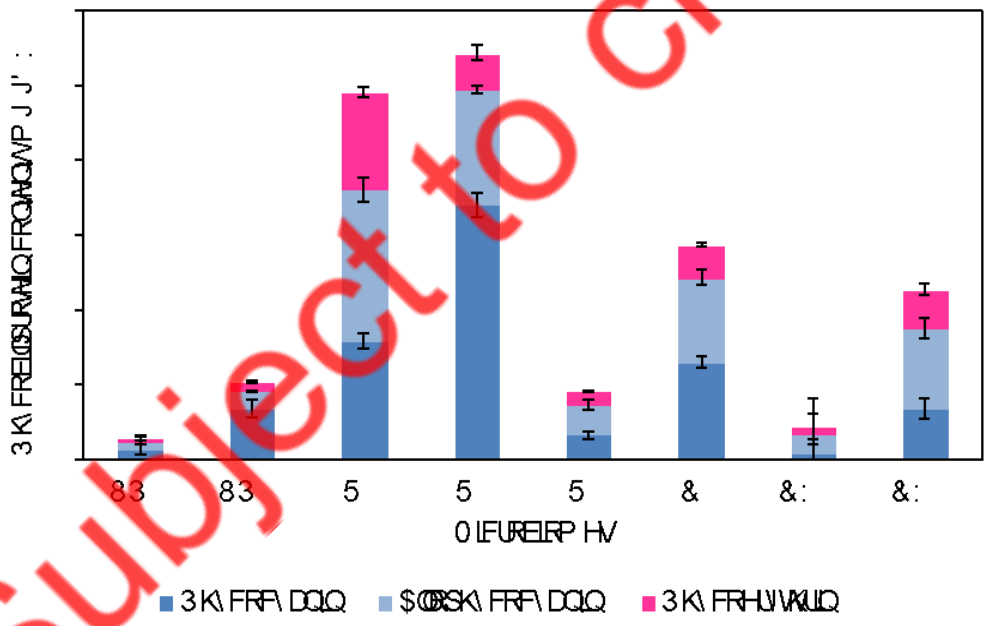

Figure 20: Phycobiliproteins results of the different cyanobacteria microbiomes. a) Image of phycobiliproteins after extraction. b) Phycobiliprotein content results. Values represent the average and standard deviation (error bars) of 3 replicates.

The amount of PPP was in general low except for samples R 1 and R 2, which at the same time were those with the lower PHA content. Interestingly, these samples were much rich in filamentous cyanobacteria, *Synechocystis* sp. and cf. *Gloeobacter* sp. On the other hand, sample UP 3, in which filamentous cyanobacteria and green algae were observed, presented the low PPP content. Although samples R 1 and R 2 exhibit the higher PPP content (mg/gDW), note that the color of sample R 1 is orange and the R 2 is greener

(Figure 20a), this could be explained by the different composition of PC, APC and PE in this samples.

The amount of PC and APC was similar in all samples, while the content in PE was lower. Previous experience of the UPC partner in the production of PPP in *Synechocystis* sp*. and Synechococus* sp. monocultures showed a very different pigment proportion; being PC the higher produced pigment and APC and PE the lower ones.

2.4.3 Carotenoids

For the extraction of carotenoids, the procedures reported by Zavřel et al. (2015) were adapted for this study. Freeze-dried biomass (~ 3 mg) was used to extract carotenoids. Biomass was then distributed in 1.5 mL tubes, and 1 mL of methanol (4ºC) was added per sample. Firstly, mixtures were homogenized by vortexing (2000 rpm, 4 sec) (Vortex-Genie™ 2, Scientific Industries SI™) and covered with aluminum foil. Samples were incubated at 4 °C for 20 min, and then centrifuged (15000 xg, 4°C) for 7 min. If the pellets remained green, samples were vortexed and incubated again. Pellets were recovered, and carotenoid concentrations were measured in a plate reader (Synergy™ HT, BioTek) at OD_470nm, OD_665nm and OD_720nm. Methanol was used as a blank. The concentrations of carotenoids and chlorophyll a (Chla) were quantified according to the following equations:

- Chla [µg/ml] = 12.9447 (A_665 – A_720) (Ritchie, 2006)
- Carotenoids [µg/ml] = [1,000 (A_470 – A_720) − 2.86 (Chla [µg/ml])] / 221 (Wellburn, 1994).

All the analyses were performed in triplicates and under dark conditions to avoid pigment degradation. Results are shown in Figure 21.

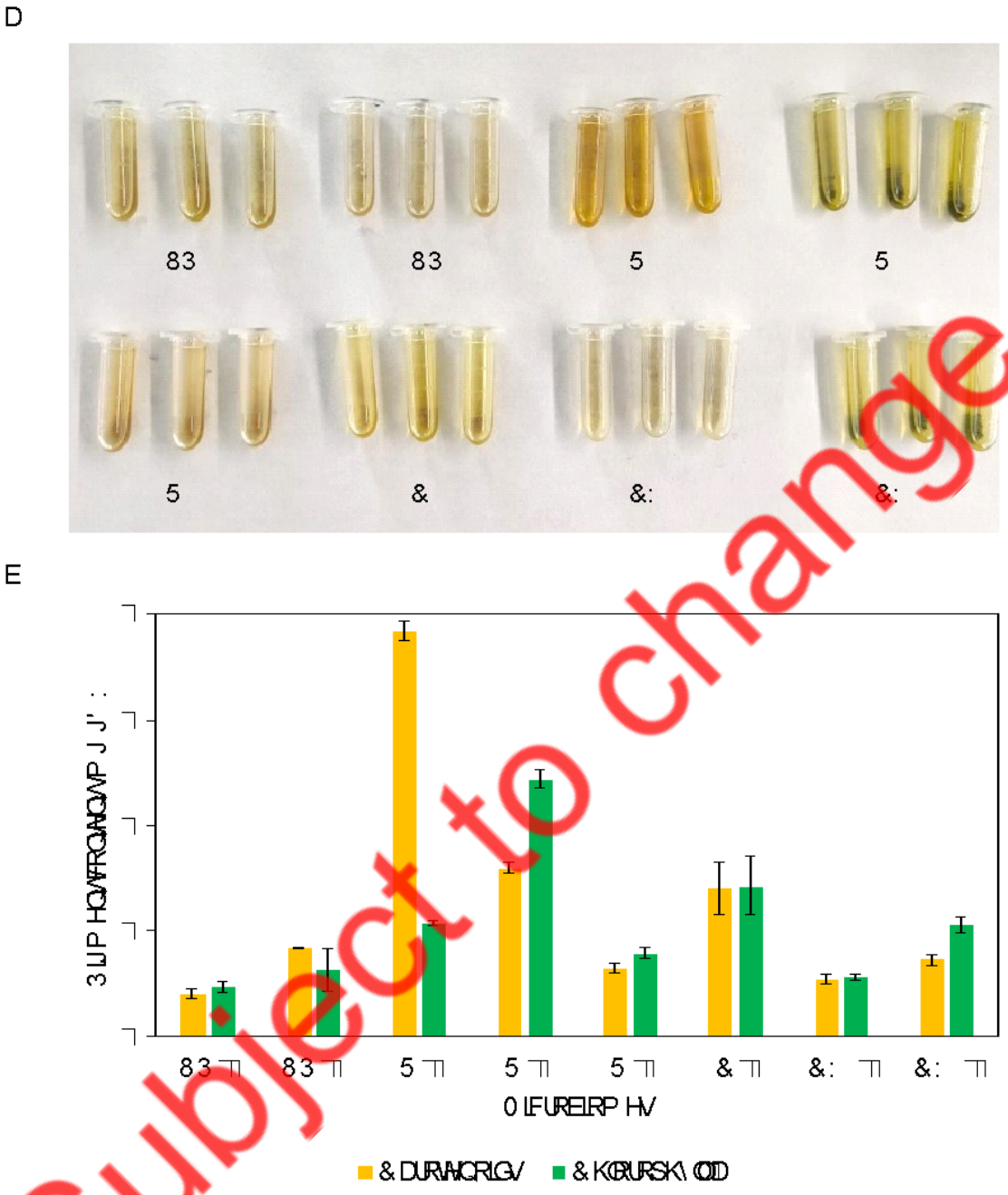

Figure 21: Carotenoids analysis of the different cyanobacteria microbiomes. a) Image of carotenoids after extraction. b) Carotenoids content analysis. Values represents the average and standard deviation (error bars) of 3 replicates.

In connection with the PPP results, the samples which had higher amount of carotenoids were R 1 and R 2. Also, the samples with lower content of carotenoids were those with lower PPP (UP 3 and CW 1).

2.4.4 Extracellular Polysaccharides (EPS)

For the EPS compositional analysis, a sample of 15 ml of culture broth was centrifuged (4,400 rpm for 10 min). 4% NaCl and two volumes of 96% cold ethanol were added to the

cell-free supernatant, followed by centrifugation (7,000 rpm, 12 min) in order to facilitate EPS precipitation. The pellet was diluted in 5mL deionized water and freeze dried.

Freeze-dried samples (~5 mg) were dissolved in deionized water (5 mL) and hydrolyzed with 0.1 mL 99% trifluoroacetic acid (TFA) at 120 °C for 4 h. The hydrolysate was used for the identification and quantification of the constituent sugar monomers and uronic acids by anion exchange chromatography, using a Metrosep Carb 2 - 250/4.0 column (Metrohm, AG), equipped with a pulsed amperometric detector. The eluents used were (A) 1 mM sodium hydroxide and 1 mM sodium acetate and (B) 300 mM sodium hydroxide and 500 mM sodium acetate. The analysis was performed at 30 °C, at a flow rate of 0.6 mL/min. Results of the total EPS content for each microbiome and EPS composition is shown in Table 9.

Table 9: EPS content and composition of the different cyanobacteria microbiomes.

Sugar monomer (mg/L)	UP 3	UP 4	R 1	R 2	R 3	C 2	CW 1	CW 2
Fucose	0.41	0.27	2.61	0.82	1.23	1.32	0.40	1.37
Galactose	0.27	1.11	3.17	0.64	2.69	3.62	0.96	1.30
Arabinose	0.31	0.75	0.31	0.44	1.06	0.35	0.31	0.63
Glucose	0.02	1.94	4.00	1.32	5.53	9.91	0.38	1.82
Rhamnose	0.48	0.77	1.74	0.77	1.82	3.53	0.57	2.86
Xylose	0.16	0.63	1.58	0.62	1.60	1.26	0.23	0.98
Mannose	0.37	0.78	0.85	0.67	2.39	2.62	0.53	0.71
Fructose	0.16	0.15	0.47	0.00	0.03	0.00	0.00	0.00
Galacturonic acid	0.00	0.00	0.14	0.00	0.59	0.45	0.02	0.08
Glucuronic acid	0.02	0.06	0.31	0.02	0.15	0.58	0.06	0.18
Total	**2.19**	**6.46**	**15.17**	**5.30**	**17.10**	**23.63**	**3.47**	**9.93**

The higher concentration of EPS was achieved in samples C 2, R 3 and R 1. Interestingly, the microscopic observation of this samples revealed a composition of filamentous and punctiform colonial cyanobacteria as major abundant microorganisms. On the other hand, glucose was the most produced monomer, followed by galactose and rhamnose.

2.4.5 Microbiome bioproduct productivity

Figure 22 is intended to sum up the developed cyanobacteria microbiomes with their productivity for PHA, PPP carotenoids, and EPS bioproducts. Samples R 1 and R 2 exhibited the highest PPP and carotenoid expression and were at the same time the ones with lowest PHA percentages. On the other hand, samples R 3 and UP 4 contain the highest PHA percentages and lowest PPP and carotenoids expression, however sample R 3 produced an interesting concentration of EPS. Otherwise, C 2 microbiome produced the higher concentration of EPS with a moderate (> 50%) production of PHA, PPP and carotenoids.

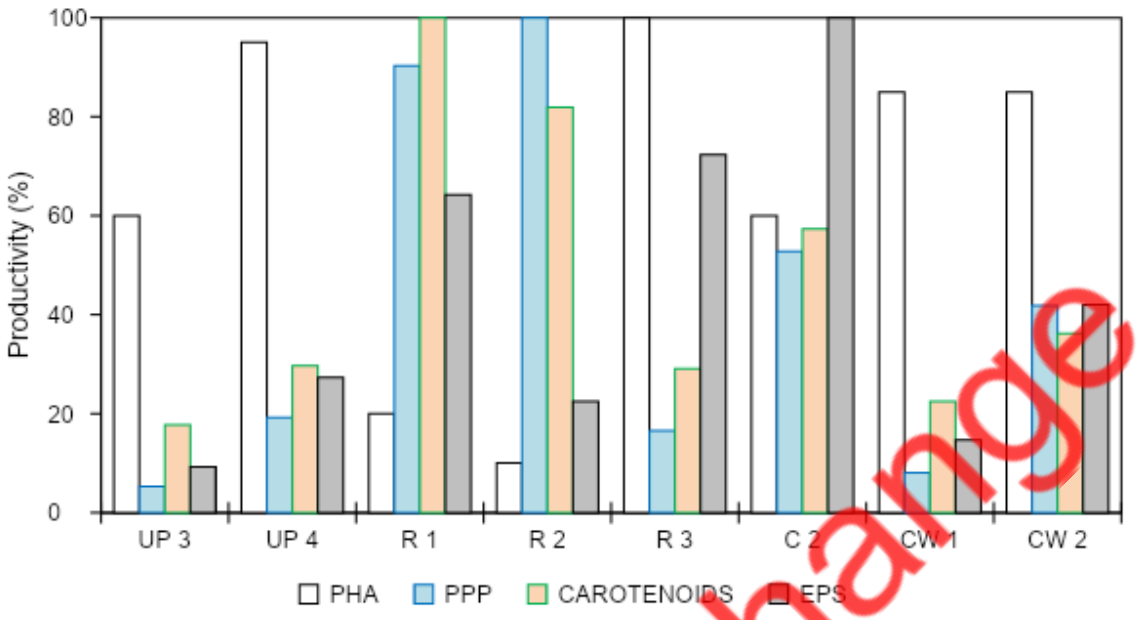

Figure 22: Productivity production percentage of the different bioproducts by cyanobacteria microbiomes. Productivity was obtained by normalizing each bioproduct concentration by its maximum. Bars show the relative percentage productivities for each bioproduct. Samples UP 1, UP 2 and C 1 were discarded during nutrient selection phase.

2.5 16s rRNA Microbiome characterization

Microbiome characterization by means of 16s rRNA was performed following two different strategies to gain a deeper knowledge on the impact of the nutritional pressor over the microbial community. Therefore, two sets of samples were analysed: (i) raw environmental samples C 1 and CW 2, and (ii) selected cyanobacteria microbiomes for UP 1-4 and R 1-3 samples. As previously presented in Section 2.2.1 we collected samples from environmental microbiomes containing a variety of microorganisms. Then, we forced our samples under selective pressure to obtain the cyanobacteria enriched microbiomes consisting of mixed populations of cyanobacteria and other organisms such as heterotrophic bacteria. Hence, microbiomes resulting from nutrient selection were the candidates for bioproduct and microbiome characterization.

After quality and chimeric sequence filtering 443.627 reads were obtained (55.543 ±6.740 per sample). The reads were grouped into 1543 bacterial amplicon sequence variant (ASVs). We calculated a rarefaction curve (alpha-diversity index) for all the samples at the ASV taxonomic level to evaluate the sequencing deep rightness. The samples reached the plateau area (Figure 23), so an increase in the number of sequences must not impact the number of ASVs detected.

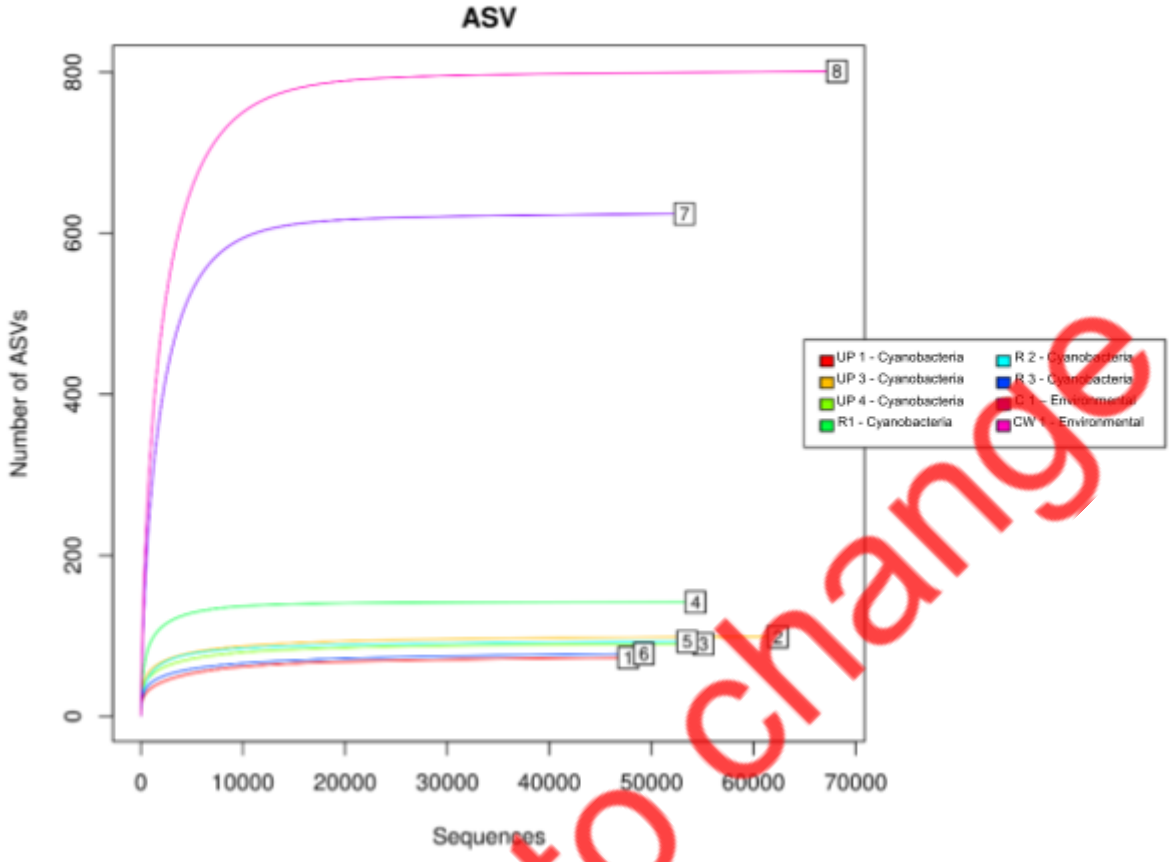

Figure 23: Rarefaction curves of bacterial population at ASV taxonomic level.

As can be observed in Figure 23, the number of ASV detected in the natural environmental samples was much higher than those of samples with selected microbiomes, reflecting a much lower diversity due to the selective pressure.

The 1543 ASVs belonged to 12 different phyla, being the most abundant Cyanobacteria (25.91 ± 10.15%), Bacteroidetes (27.78 ± 10.60%), and Proteobacteria (27.22 ± 6.51%) (Figure 24). As can be observed, the selective pressure allowed to maintain high abundances of cyanobacteria which are the target organisms for the purpose of the project.

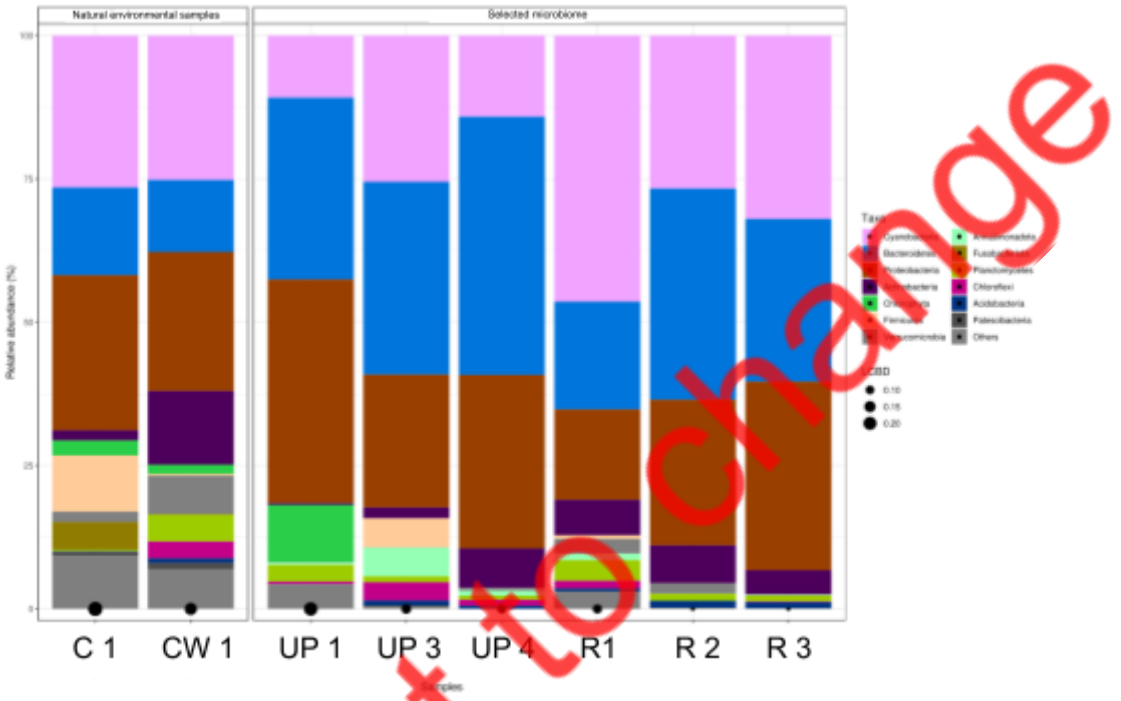

Figure 24: Relative abundances of the phyla and the LCBD values of all the samples. The label others represent the unknowns.

Families with the highest relative abundance across all the samples were Flavobacteriaceae (Phylum: Bacteroidetes) (17.67 ± 13.24%), Cyanobiaceae (Phylum: Cyanobacteria) (4.50 ± 6.27%), and Rhodanobacteraceae (Phylum: Proteobacteria) (6.24 ± 7.80%) (Fgure 24). We observed a relative abundance increment of Cyanobiaceae family in several samples of selected microbiome group respect the environmental ones (Figure 25).

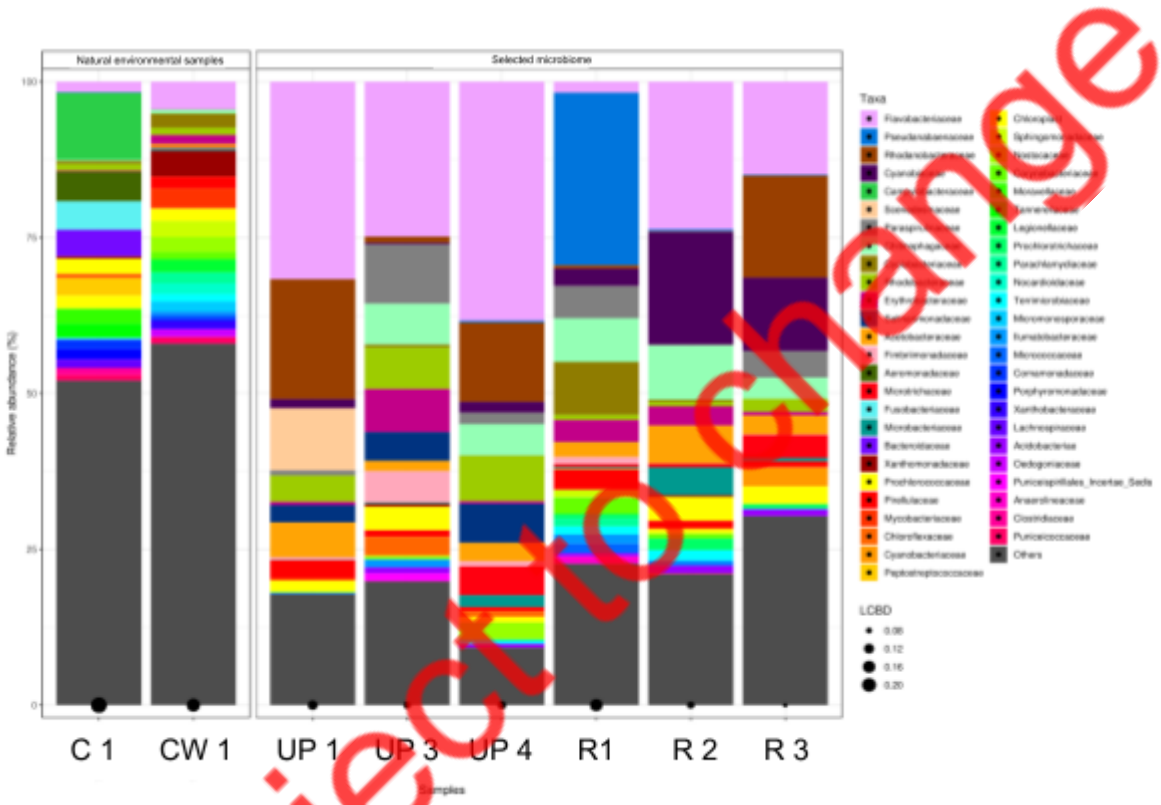

Figure 25: Relative abundances of the 62 most abundant families and the LCBD values of all the samples. The label others represent the rest of the families, including the unknowns.

A total of 427 genera were detected, 23 of them belonging to Cyanobacteria phylum (Table 10).

Table 10: List of genera belonged to Cyanobacteria phylum

Genera belonging to Cyanobacteria phylum	
Pseudanabaena_PCC 7403	*Albertania*
Prochlorococcus_MIT9313	*Oculatella*
Prochlorococcus	*Foliisarcina*
Nodosilinea	*Cyanobacterium*
Cyanobacterium_PCC 10605	*Gastranaerophilales*
Sphaerospermopsis_BCCUSP55	*Calochaete*

Cyanobium	*Pegethrix*
Nostoc	*Synechococcus*
Atlanticothrix	*Caenarcaniphilales*
Microcystis_PCC 7914	*Sericytochromatia*
Pleurocapsa	*Tildeniella*
Altericista	

The most abundant genera were: *Flavobacterium* (Phylum: Bacteroidetes) (17.25 13.70%), *Prochlorococcus*_MIT9313 (Phylum: Cyanobacteria) (4.24 ± 6.41%), *Aquimonas* (Phylum: Proteobacteria) (3.74 ± 6.82%), and *Pseudanabaena*_PCC 7403 (Phylum: Cyanobacteria) (3.57 ± 9.12%) (Figure 26).

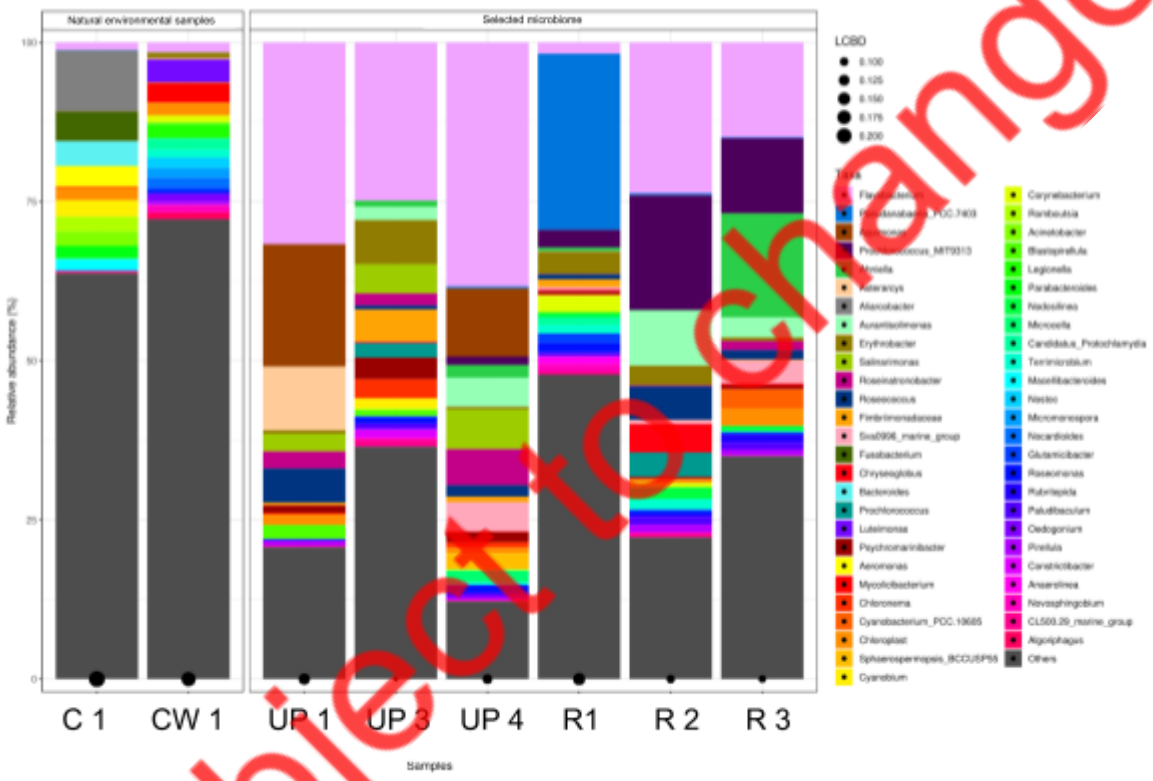

Figure 26: Relative abundances of the 62 most abundant genera and the LCBD values of all the samples. The label others represent the rest of the genera, including the unknowns.

The most abundant ASVs detected were: ASV1[5]*Flavobacterium* (16.01 ± 13,65%), ASV8[5]*Pseudanabaena*_PCC 7403 (3.42 ± 8.94%), ASV12[2]Alphaproteobacteria (3.21 ± 3.72%), ASV14[6]*Aquimonas voraii* (3.02 ± 6.20%), and ASV13[5]*Prochlorococcus*_MIT9313 (2.91 ± 5.53%) (Figure 27). At his taxonomic level we observed highest abundance of: ASV1[5]*Flavobacterium* in the selected microbiome samples group than in the natural environmental sample group.

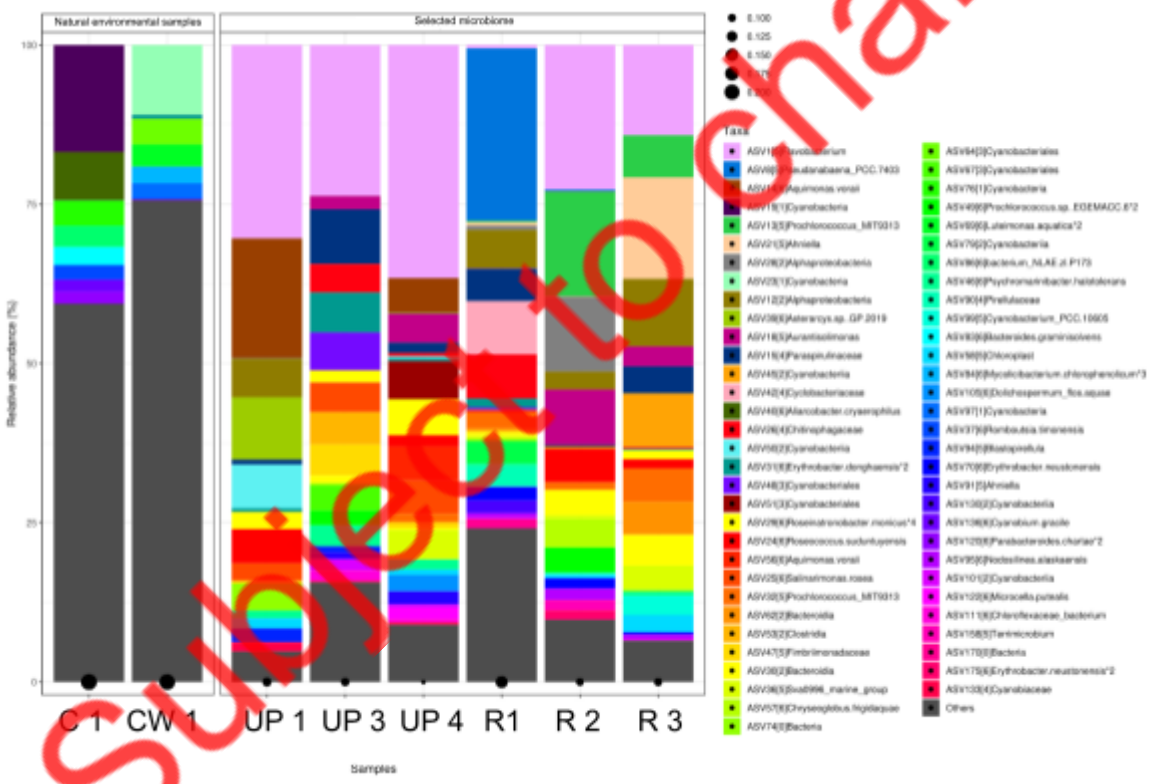

Figure 27: Relative abundances of the 62 most abundant ASVs and the LCBD values of all the samples. The label others represent the rest of the ASVs.

To analyse de alpha diversity Richness, Shannon and Simpson metrics, the metrics were significantly higher in natural environmental group compared to selected microbiome group (Figure 28).

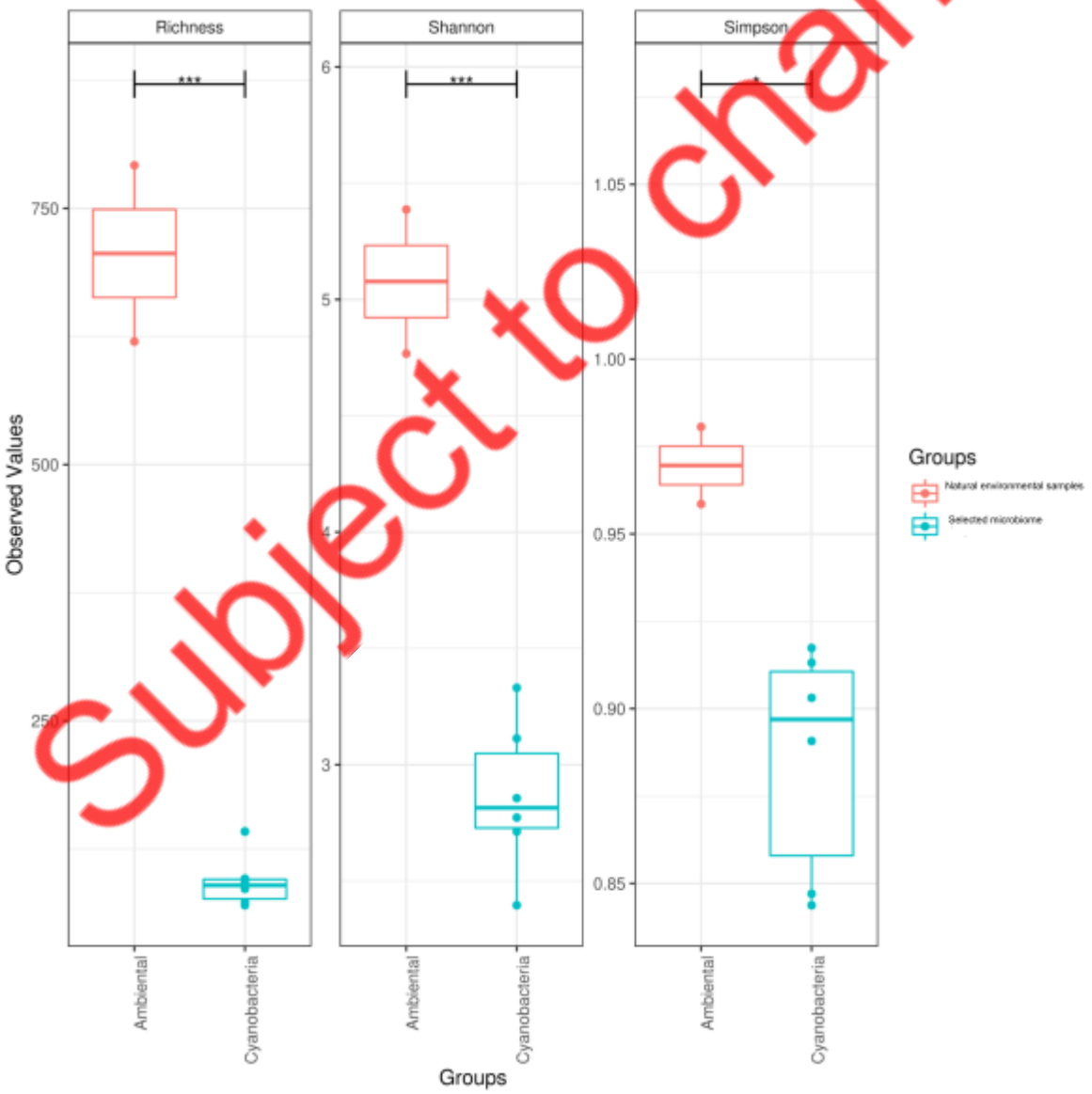

Figure 28: ASVs diversity of the microbiome of each group. Number of samples analysed per group: natural environmental samples:2 and selected microbiome:2. (*) indicate significant differences between groups according to ANOVA tests ($p < 0.05$).

As expected, the raw environmental samples had much higher diversity than the selected microbiomes.

3 Conclusions

Microbiomes originating from a variety of sites were collected. After a preliminary characterization of the environmental samples, selection assays were conducted to enrich the microbiomes in PHA, EPS and/or PPP.

NOVA.id has imposed the environmental samples to feast-and-famine alternate cycles for the selection of PHA-storing microorganism. All microbiomes evolved into communities containing PHA-accumulating organisms, with the samples originating from the river marshland and the forest soils yielding higher PHA content. Since the same metabolic pressure was imposed to the all the original microbiomes, the selection of microbial communities with different abilities to produce PHA was a consequence of the microbial composition of the initial microbiome. Despite the applied conditions not being specific for selecting EPS producers, all strains secreted EPS of distinct composition, with the highest production attained by the forest soil selected microbiomes, and the one from the dune plant root.

UPC has conducted a selection based on P limitation to obtain microbiomes rich in cyanobacteria. After this selection phase, several cyanobacteria-containing microbiomes were obtained and bioproducts were analyzed. Samples R 1 and R 2 exhibit the highest phycobiliprotein and carotenoid expression whereas they the ones with lowest PHA percentages. On the other hand, samples R 3 and UP 4 contained the highest PHA percentages. The bioproduct screening allowed to see the potential of the collected microbiomes, resulting on samples R 1-3 and UP 4 the most promising.

Future work in PROMICON project will be devoted on defining and implementing the optimal conditions for each bioproduct production, as well as their physical-chemical and functional characterization.

4 References

16S Metagenomic Sequencing Library Preparation Protocol. (ILLUMINA).

Albuquerque, M.G., Torres, C.A.V., Reis, M.A.M. 2010. Polyhydroxyalkanoate (PHA) production by a mixed microbial culture using sugar molasses: Effect of the influent substrate concentration on culture selection. Water research 44: 3419 – 3433. doi:10.1016/j.watres.03.021.

Albuquerque M.G., Martino V., Pollet E., Avérous L., Reis M.A.M. 2011. Mixed culture polyhydroxyalkanoate (PHA) production from volatile fatty acid (VFA)-rich streams: effect of substrate composition and feeding regime on PHA productivity, composition and properties. J Biotechnol. 151(1):66-76. doi:10.1016/j.jbiotec.2010.10.070

Altschul, S.F., Gish, W., Miller, W., Myers, E.W. and Lipman, D.J. 1990. Basic local alignment search tool. J. Mol. Biol. 215:403-410.

Amann, R.I., Binder, B.J., Olson, R.J., Chisholm, S.W., Devereux, R., Stahl, D.A. 1990. Combination of 16S rRNA-targeted oligonucleotide probes with flow cytometry for analyzing mixed microbial populations. Appl Environ Microbiol. 56(6):1919-1925. doi:10.1128/aem.56.6.1919-1925.1990

Andersen, R.A., 2005. Algal Culturing Techniques, Elsevier. Ed

APHA, 1995. Standard Methods for the Examination of Water and Wastewater, American Public Health Association, Washington DC.

APHA, AWWA, WEF, 2012. Standard methods for the examination of water and wastewater. Stand. Methods, 541

Arias, D.M., García, J., Uggetti, E., 2020. Production of polymers by cyanobacteria grown in wastewater: current status, challenges and future perspectives. N. Biotechnol. 55, 46-57

Aullybux, A.A., Puchooa, D., Bahorun, T., Jeewon, R. 2019. Phylogenetics and antibacterial properties of exopolysaccharides from marine bacteria isolated from Mauritius seawater. *Ann Microbiol* 69, 957–972. https://doi.org/10.1007/s13213-019-01487-2

Bolyen E., Rideout J.R., Dillon, M.R., et al. 2019. Reproducible, interactive, scalable and extensible microbiome data science using QIIME 2 [published correction appears in Nat Biotechnol. 2019 Sep;37(9):1091]. Nat Biotechnol. 37(8):852-857. doi:10.1038/s41587-019-0209-9

Cruz MV, Araujo D, Alves VD, Freitas F, Reis MAM. 2016. Characterization of medium chain length polyhydroxyalkanoate produced from olive oil deodorizer distillate. Int J Biol Macromol. 82: 243-248. doi:10.1016/j.ijbiomac.2015.10.043

Daims, H., Brühl, A., Amann, R., Schleifer, K.H., Wagner, M. 1999. The domain-specific probe EUB338 is insufficient for the detection of all Bacteria: development and evaluation of a more comprehensive probe set. Syst Appl Microbiol. 22(3):434-444. doi:10.1016/S0723-2020(99)80053-8

Ferreira, A., Torres, C.A.V., Freitas, F., Sevrin, C., Grandfils, C., Reis, M.A.M. 2016. Alves VD, Coelhoso IM Development and characterization of bilayer films of FucoPol and chitosan. Carbohydr. Polym. 8-15. doi:10.1016/j.carbpol.2016.03.089

Fradinho, J., Carvalho, G., Oehmen, A., Reis, M.A.M., 2013. Determination of the extraction kinetics for the quantification of polyhydroxyalkanoate monomers in mixed microbial systems. Process Biochem. 48, 1626–1634.

Greuter, D., Loy, A., Horn, M., Rattei, T. 2016. probeBase--an online resource for rRNA-targeted oligonucleotide probes and primers: new features. Nucleic Acids Res. 44(D1): D586-D589. doi:10.1093/nar/gkv1232

Grigoryeva Yu, N., 2020. Studying Cyanobacteria by Means of Fluorescence Methods: A Review Natalia Yu. Fluorescence Methods for Investigation of Living Cells and Microorganisms, 9. DOI: 10.5772/intechopen.93543

Joulak, I., Concórdio-Reis, P., Torres, C.A.V., Sevrin, C., Grandfils, C., Attia, H., Freitas, F. Reis, M.A.M., Azbou, S. 2021. Sustainable use of agro-industrial wastes as potential feedstocks for exopolysaccharide production by selected *Halomonas* strains. Environ Sci Pollut Res . https://doi.org/10.1007/s11356-021-17207-w

Klindworth, A., Pruesse, E., Schweer, T., Peplies, J., Quast, C., Horn, M., Glöckner, F.O. 2013. Evaluation of general 16S ribosomal RNA gene PCR primers for classical and next-generation sequencing-based diversity studies. Nucleic Acids Res. 41(1):e1. doi: 10.1093/nar/gks808.

Komárek, J., Hauer, T., [WWW Document]. http://www.cyanodb.cz. 2013. Cyan- oDB.cZ - On-line Database of Cyanobacterial Genera. - Word-wide Electronic Publication Univ. South Bohemia Inst. Bot. AS CR.

Lanham, A.B., Rita, A., Albuquerque, M.G.E., Pardelha, F., Carvalheira, M., Coma, M.,Fradinho, J., Carvalho, G., Oehmen, A., Reis, M.A.M. 2014 Determination of the extraction kinetics for the quantification of polyhydroxyalkanoate monomers in mixed microbial systems. Process Biochemistry 48(11): 1626-1634. DOI: 10.1016/j.procbio.2013.07.023

Loy, A., Lehner, A., Lee, N., Adamczyk, J., Meier, H., Ernst, J., Schleifer, K.H., Wagner, M., 2002. Oligonucleotide microarray for 16S rRNA gene-based detection of all recognized lineages of sulfate-reducing prokaryotes in the environment. Appl Environ Microbiol. 68(10):5064-5081. doi:10.1128/AEM.68.10.5064-5081.2002

Ma, W., Wang, J., Li, Y., Yin, L., Wang, X. *2018*. Poly(3-hydroxybutyrate-co-3-hydroxyvalerate) co-produced with L-isoleucine in *Corynebacterium glutamicum* WM001. *Microb Cell Fact* 17, 93. https://doi.org/10.1186/s12934-018-0942-7

Manz, W., Amann, R., Ludwig, W., Wagner, M., Schleifer, K.-H. 1992. Phylogenetic Oligodeoxynucleotide Probes for the Major Subclasses of Proteobacteria: Problems and Solutions. Syst. Appl. Microbiol. 15:593–600. doi:10.1016/S0723-2020(11)80121-9.

Manz, W., Amann ,R., Ludwig, W., Wagner M., and Schleifer K.H. 1996. Application of a suite of 16S rRNA-specific oligonucleotide probes designed to investigate bacteria of the phylum cytophaga-flavobacter-bacteroides in the natural environment. Microbiology. 142:1097-1106. doi:10.1099/13500872-142-5-1097

Martin, M. 2011. Cutadapt removes adapter sequences from high- throughput sequencing reads. EMBnet .journal 17(1):10-12.

Meier, H., Amann, R., Ludwig, W., Schleifer, K.H. 1999. Specific oligonucleotide probes for in situ detection of a major group of gram-positive bacteria with low DNA G + C content. Syst Appl Microbiol. 22(2):186-196. doi:10.1016/S0723-2020(99)80065-4

Nielsen, P.H., Daims, H., Lemmer, H., 2009. FISH Handbook for Biological Wastewater Treatment: Identification and Quantification of Microorganisms in Activated Sludge and Biofilms by FISH. IWA Publishing Company, London

Oehmen, A., Zeng, R.J., Saunders, A.M., Blackall, L.L., Keller, J., Yuan, Z. 2006. Anaerobic and aerobic metabolism of glycogen-accumulating organisms selected with propionate as the sole carbon source. Microbiology (Reading). 152(9):2767-2778. doi:10.1099/mic.0.28065-0

Oksanen, J., Blanchet, F.G., Friendly, M., Kindt, R. , et al. 2019. vegan: Community Ecology Package. R package version 2.5-6. https://CRAN.R-project.org/package=vegan

Palmer, C.M., Tarzwell, C., Walter, H.J., Falcón de Gyves, C., Guerrero Torres, R., 1962. Algas En Abastecimientos De Agua: Manual Ilustrado Acerca De La identificación, Importancia Y Control De Las Algas En Los Abastecimientos De Agua, Centro Reg. Ed. Mexico city

R Development Core Team (2008). R: A language and environment for statistical computing. R Foundation for Statistical Computing, Vienna, Austria. ISBN 3-900051-07-0, URL http://www.R-project.org.

Rains, D. W., Schmid, W.E., Epstei, E. 1964. Absorption of Cations by Roots. Effects of Hydrogen Ions and Essential Role of Calcium. Plant Physiology 39(2), American Society of Plant Biologists (ASPB): 274–78. http://www.jstor.org/stable/4260205

Rebocho, A.T., Pereira, J.R., Freitas, F., Neves, L.A., Alves, V.D., Sevrin, C., Grandfils, C., Reis, M.A.M. 1995. Production of medium-chain lenucleic acid probes. Molecular Microbial Ecology Manual. Springer, Dordrecht. 331-345. doi:10.1007/978-94-011-0351-0_23

Roller, C., Wagner, M., Amann, R., Ludwig, W., Schleifer, K.H. 1995. *In situ* probing of gram-positive bacteria with high DNA G + C content using 23S rRNA-targeted oligonucleotides [published correction appears in Microbiology. 1995 May;141 (Pt 5):1267]. Microbiology (Reading). 140 (10):2849-2858. doi:10.1099/00221287-140-10-2849

Sakan, S., Franciskovic-Bilinski, S., Dordevic, D., Popovic, A., Sakan, N., Skivanj, S., Bilinski, H. 2021. Evaluation of Element Mobility in River Sediment Using Different Single Extraction Procedures and Assessment of Probabilistic Ecological Risk. Water 13(10) 1411. https://doi.org/10.3390/w13101411

Shannon, C.E. 1948. A mathematical theory of communication. The Bell System Technical Journal, 27, 379–423 and 623–656.

Silvestre ,S.L., Araújo, D., Marques, A.C., Pires, C., Matos, M., Alves, V., Martins, R., Freitas, F., Reis, M.A.M., Fortunato, E. 2020. Microneedle arrays of polyhydroxyalkanoate by laser-based micromolding technique. ACS Appl. Bio Mater. 3(9) 5856-5864. doi:10.1021/acsabm.0c00570

Simpson, E. Measurement of Diversity. 1949. Nature 163, 688. https://doi.org/10.1038/163688a0

Stanley, A., Kumar, H.N.P., Mutturi, S., Vijayendra, S.V.N. 2018. Fed-Batch Strategies for Production of PHA Using a Native Isolate of *Halomonas venusta* KT832796 Strain. Appl Biochem Biotechnol 184(3): 935–952. https://doi.org/10.1007/s12010-017-2601-6

Streble, H., Krauter, D., 2018. Das Leben Im Wassertropfen: Mikroflora Und Mikrofauna Des Süsswassers. Kosmos, veränd. Aufl. Edition, Stuttgart

Sutherland, D.L., Turnbull, M.H., Craggs, R.J. 2017. Environmental drivers that influence microalgal species in fullscale wastewater treatment high rate algal ponds. Water research 124, 504-512. 10.1016/j.watres.2017.08.012

Tan, W.A., Wijaya, I., Purwadaria, T. 2019. Bioprospecting of polyhydroxyalkanoates-producing bacteria from Indonesian marine environment. Biodiversitas 20(5): 1309-1315. DOI: 10.13057/biodiv/d20052

Venkateswar Reddy, M., Mawatari, Y., Onodera, R., Nakamura, Y., Yajima, Y., Chang, Y.C., 2017. Polyhydroxyalkanoates (PHA) production from synthetic waste using *Pseudomonas pseudoflava*: PHA synthase enzyme activity analysis from *P. pseudoflava* and *P. palleronii*. Bioresour. Technol. 234, 99–10, DOI: 10.1016/j.biortech.2017.03.008

Weiss, S., Xu, Z.Z., Peddada, S., Amir, A., Bittinger, K., Gonzalez, A., Lozupone, C., Zaneveld, J.R., Vázquez-Baeza, Y., Birmingham, A., Hyde, E.R., Knight, R. 2017. Normalization and microbial differential abundance strategies depend upon data characteristics. Microbiome 5(27). DOI 10.1186/s40168-017-0237-y

Yadav, K.K., Mandal, A.K., Sen, I.K., Chakraborti, S., Islam, S.S., Chaktaborty R. 2012. Flocculating Property of Extracellular Polymeric Substances Produced by a Biofilm-Forming Bacterium *Acinetobacter junii* BB1A. Appl Biochem Biotechnol 168, 1621–1634. https://doi.org/10.1007/s12010-012-9883-5

Zheng,Y., Guo, L., Liu, Y., She, Z., Gao, M., Jin, C., Zhao, Y. 2021.Effects of chemical oxygen demand concentration, pH and operation cycle on polyhydroxyalkanoates synthesis with waste sludge. Environmental Technology 42:12, pages 1922-1929. doi.org/10.1080/09593330.2017.1330902

16S Metagenomic Sequencing Library Preparation Protocol. (ILLUMINA).

Albuquerque, M.G., Torres, C.A.V., Reis, M.A.M. 2010. Polyhydroxyalkanoate (PHA) production by a mixed microbial culture using sugar molasses: Effect of the influent substrate concentration on culture selection. Water research 44: 3419 – 3433. doi:10.1016/j.watres.03.021.

Albuquerque M.G., Martino V., Pollet E., Avérous L., Reis M.A.M. 2011. Mixed culture polyhydroxyalkanoate (PHA) production from volatile fatty acid (VFA)-rich streams: effect of substrate composition and feeding regime on PHA productivity, composition and properties. J Biotechnol. 151(1):66-76. doi:10.1016/j.jbiotec.2010.10.070

Altschul, S.F., Gish, W., Miller, W., Myers, E.W. and Lipman, D.J. 1990. Basic local alignment search tool. J. Mol. Biol. 215:403-410.

Amann, R.I., Binder, B.J., Olson, R.J., Chisholm, S.W., Devereux, R., Stahl, D.A. 1990. Combination of 16S rRNA-targeted oligonucleotide probes with flow cytometry for analyzing mixed microbial populations. Appl Environ Microbiol. 56(6):1919-1925. doi:10.1128/aem.56.6.1919-1925.1990

Andersen, R.A., 2005. Algal Culturing Techniques, Elsevier. Ed

APHA, 1995. Standard Methods for the Examination of Water and Wastewater, American Public Health Association, Washington DC.

APHA, AWWA, WEF, 2012. Standard methods for the examination of water and wastewater. Stand. Methods, 541

Arias, D.M., García, J., Uggetti, E., 2020. Production of polymers by cyanobacteria grown in wastewater: current status, challenges and future perspectives. N. Biotechnol. 55, 46-57

Aullybux, A.A., Puchooa, D., Bahorun, T., Jeewon, R. 2019. Phylogenetics and antibacterial properties of exopolysaccharides from marine bacteria isolated from Mauritius seawater. *Ann Microbiol* 69, 957–972. https://doi.org/10.1007/s13213-019-01487-2

Bolyen E., Rideout J.R., Dillon, M.R., et al. 2019. Reproducible, interactive, scalable and extensible microbiome data science using QIIME 2 [published correction appears in Nat Biotechnol. 2019 Sep;37(9):1091]. Nat Biotechnol. 37(8):852-857. doi:10.1038/s41587-019-0209-9

Cruz MV, Araujo D, Alves VD, Freitas F, Reis MAM. 2016. Characterization of medium chain length polyhydroxyalkanoate produced from olive oil deodorizer distillate. Int J Biol Macromol. 82: 243-248. doi:10.1016/j.ijbiomac.2015.10.043

Daims, H., Brühl, A., Amann, R., Schleifer, K.H., Wagner, M. 1999. The domain-specific probe EUB338 is insufficient for the detection of all Bacteria: development and evaluation of a more comprehensive probe set. Syst Appl Microbiol. 22(3):434-444. doi:10.1016/S0723-2020(99)80053-8

Ferreira, A., Torres, C.A.V., Freitas, F., Sevrin, C., Grandfils, C., Reis, M.A.M. 2016. Alves VD, Coelhoso IM Development and characterization of bilayer films of FucoPol and chitosan. Carbohydr. Polym. 8-15. doi:10.1016/j.carbpol.2016.03.089

Fradinho, J., Carvalho, G., Oehmen, A., Reis, M.A.M., 2013. Determination of the extraction kinetics for the quantification of polyhydroxyalkanoate monomers in mixed microbial systems. Process Biochem. 48, 1626–1634.

Greuter, D., Loy, A., Horn, M., Rattei, T. 2016. probeBase--an online resource for rRNA-targeted oligonucleotide probes and primers: new features. Nucleic Acids Res. 44(D1): D586-D589. doi:10.1093/nar/gkv1232

Grigoryeva Yu, N., 2020. Studying Cyanobacteria by Means of Fluorescence Methods: A Review Natalia Yu. Fluorescence Methods for Investigation of Living Cells and Microorganisms, 9. DOI: 10.5772/intechopen.93543

Joulak, I., Concórdio-Reis, P., Torres, C.A.V., Sevrin, C., Grandfils, C., Attia, H., Freitas, F. Reis, M.A.M., Azbou, S. 2021. Sustainable use of agro-industrial wastes as potential feedstocks for exopolysaccharide production by selected *Halomonas* strains. Environ Sci Pollut Res . https://doi.org/10.1007/s11356-021-17207-w

Klindworth, A., Pruesse, E., Schweer, T., Peplies, J., Quast, C., Horn, M., Glöckner, F.O. 2013. Evaluation of general 16S ribosomal RNA gene PCR primers for classical and next-generation sequencing-based diversity studies. Nucleic Acids Res. 41(1):e1. doi: 10.1093/nar/gks808.

Komárek, J., Hauer, T., [WWW Document]. http://www.cyanodb.cz. 2013. Cyan- oDB.cZ - On-line Database of Cyanobacterial Genera. - Word-wide Electronic Publication Univ. South Bohemia Inst. Bot. AS CR.

Lanham, A.B., Rita, A., Albuquerque, M.G.E., Pardelha, F., Carvalheira, M., Coma, M.,Fradinho, J., Carvalho, G., Oehmen, A., Reis, M.A.M. 2014 Determination of the extraction kinetics for the quantification of polyhydroxyalkanoate monomers in mixed microbial systems. Process Biochemistry 48(11): 1626-1634. DOI: 10.1016/j.procbio.2013.07.023

Loy, A., Lehner, A., Lee, N., Adamczyk, J., Meier, H., Ernst, J., Schleifer, K.H., Wagner, M., 2002. Oligonucleotide microarray for 16S rRNA gene-based detection of all recognized lineages of sulfate-reducing prokaryotes in the environment. Appl Environ Microbiol. 68(10):5064-5081. doi:10.1128/AEM.68.10.5064-5081.2002

Ma, W., Wang, J., Li, Y., Yin, L., Wang, X. *2018*. Poly(3-hydroxybutyrate-co-3-hydroxyvalerate) co-produced with L-isoleucine in *Corynebacterium glutamicum* WM001. *Microb Cell Fact* 17, 93. https://doi.org/10.1186/s12934-018-0942-7

Manz, W., Amann, R., Ludwig, W., Wagner, M., Schleifer, K.-H. 1992. Phylogenetic Oligodeoxynucleotide Probes for the Major Subclasses of Proteobacteria: Problems and Solutions. Syst. Appl. Microbiol. 15:593–600. doi:10.1016/S0723-2020(11)80121-9.

Manz, W., Amann ,R., Ludwig, W., Wagner M., and Schleifer K.H. 1996. Application of a suite of 16S rRNA-specific oligonucleotide probes designed to investigate bacteria of the phylum cytophaga-flavobacter-bacteroides in the natural environment. Microbiology. 142:1097-1106. doi:10.1099/13500872-142-5-1097

Martin, M. 2011. Cutadapt removes adapter sequences from high- throughput sequencing reads. EMBnet .journal 17(1):10-12.

Meier, H., Amann, R., Ludwig, W., Schleifer, K.H. 1999. Specific oligonucleotide probes for in situ detection of a major group of gram-positive bacteria with low DNA G + C content. Syst Appl Microbiol. 22(2):186-196. doi:10.1016/S0723-2020(99)80065-4

Nielsen, P.H., Daims, H., Lemmer, H., 2009. FISH Handbook for Biological Wastewater Treatment: Identification and Quantification of Microorganisms in Activated Sludge and Biofilms by FISH. IWA Publishing Company, London

Oehmen, A., Zeng, R.J., Saunders, A.M., Blackall, L.L., Keller, J., Yuan, Z. 2006. Anaerobic and aerobic metabolism of glycogen-accumulating organisms selected with propionate as the sole carbon source. Microbiology (Reading). 152(9):2767-2778. doi:10.1099/mic.0.28065-0

Oksanen, J., Blanchet, F.G., Friendly, M., Kindt, R. , et al. 2019. vegan: Community Ecology Package. R package version 2.5-6. https://CRAN.R-project.org/package=vegan

Palmer, C.M., Tarzwell, C., Walter, H.J., Falcón de Gyves, C., Guerrero Torres, R., 1962. Algas En Abastecimientos De Agua: Manual Ilustrado Acerca De La identificación, Importancia Y Control De Las Algas En Los Abastecimientos De Agua, Centro Reg. Ed. Mexico city

R Development Core Team (2008). R: A language and environment for statistical computing. R Foundation for Statistical Computing, Vienna, Austria. ISBN 3-900051-07-0, URL http://www.R-project.org.

Rains, D. W., Schmid, W.E., Epstei, E. 1964. Absorption of Cations by Roots. Effects of Hydrogen Ions and Essential Role of Calcium. Plant Physiology 39(2), American Society of Plant Biologists (ASPB): 274–78. http://www.jstor.org/stable/4260205

Rebocho, A.T., Pereira, J.R., Freitas, F., Neves, L.A., Alves, V.D., Sevrin, C., Grandfils, C., Reis, M.A.M. 1995. Production of medium-chain lenucleic acid probes. Molecular Microbial Ecology Manual. Springer, Dordrecht. 331-345. doi:10.1007/978-94-011-0351-0_23

Roller, C., Wagner, M., Amann, R., Ludwig, W., Schleifer, K.H. 1995. *In situ* probing of gram-positive bacteria with high DNA G + C content using 23S rRNA-targeted

oligonucleotides [published correction appears in Microbiology. 1995 May;141 (Pt 5):1267]. Microbiology (Reading). 140 (10):2849-2858. doi:10.1099/00221287-140-10-2849

Sakan, S., Franciskovic-Bilinski, S., Dordevic, D., Popovic, A., Sakan, N., Skivanj, S., Bilinski, H. 2021. Evaluation of Element Mobility in River Sediment Using Different Single Extraction Procedures and Assessment of Probabilistic Ecological Risk. Water 13(10) 1411. https://doi.org/10.3390/w13101411

Shannon, C.E. 1948. A mathematical theory of communication. The Bell System Technical Journal, 27, 379–423 and 623–656.

Silvestre ,S.L., Araújo, D., Marques, A.C., Pires, C., Matos, M., Alves, V., Martins, R., Freitas, F., Reis, M.A.M., Fortunato, E. 2020. Microneedle arrays of polyhydroxyalkanoate by laser-based micromolding technique. ACS Appl. Bio Mater. 3(9) 5856-5864. doi:10.1021/acsabm.0c00570

Simpson, E. Measurement of Diversity. 1949. Nature 163, 688. https://doi.org/10.1038/163688a0

Stanley, A., Kumar, H.N.P., Mutturi, S., Vijayendra, S.V.N. 2018. Fed-Batch Strategies for Production of PHA Using a Native Isolate of *Halomonas venusta* KT832796 Strain. Appl Biochem Biotechnol 184(3): 935–952. https://doi.org/10.1007/s12010-017-2601-6

Streble, H., Krauter, D., 2018. Das Leben Im Wassertropfen: Mikroflora Und Mikrofauna Des Süsswassers. Kosmos, veränd. Aufl. Edition, Stuttgart

Sutherland, D.L., Turnbull, M.H., Craggs, R.J. 2017. Environmental drivers that influence microalgal species in fullscale wastewater treatment high rate algal ponds. Water research 124, 504-512. 10.1016/j.watres.2017.08.012

Tan, W.A., Wijaya, I., Purwadaria, T. 2019. Bioprospecting of polyhydroxyalkanoates-producing bacteria from Indonesian marine environment. Biodiversitas 20(5): 1309-1315. DOI: 10.13057/biodiv/d20052

Venkateswar Reddy, M., Mawatari, Y., Onodera, R., Nakamura, Y., Yajima, Y., Chang, Y.C., 2017. Polyhydroxyalkanoates (PHA) production from synthetic waste using *Pseudomonas pseudoflava*: PHA synthase enzyme activity analysis from *P. pseudoflava* and *P. palleronii*. Bioresour. Technol. 234, 99–10, DOI: 10.1016/j.biortech.2017.03.008

Weiss, S., Xu, Z.Z., Peddada, S., Amir, A., Bittinger, K., Gonzalez, A., Lozupone, C., Zaneveld, J.R., Vázquez-Baeza, Y., Birmingham, A., Hyde, E.R., Knight, R. 2017. Normalization and microbial differential abundance strategies depend upon data characteristics. Microbiome 5(27). DOI 10.1186/s40168-017-0237-y

Yadav, K.K., Mandal, A.K., Sen, I.K., Chakraborti, S., Islam, S.S., Chaktaborty R. 2012. Flocculating Property of Extracellular Polymeric Substances Produced by a Biofilm-Forming Bacterium *Acinetobacter junii* BB1A. Appl Biochem Biotechnol 168, 1621–1634. https://doi.org/10.1007/s12010-012-9883-5

Zheng,Y., Guo, L., Liu, Y., She, Z., Gao, M., Jin, C., Zhao, Y. 2021.Effects of chemical oxygen demand concentration, pH and operation cycle on polyhydroxyalkanoates synthesis with waste sludge. Environmental Technology 42:12, pages 1922-1929. doi.org/10.1080/09593330.2017.1330902